HHS Public Access

Author manuscript

J Neurochem. Author manuscript; available in PMC 2017 December 01.

Published in final edited form as:

J Neurochem. 2016 December ; 139(5): 706–721. doi:10.1111/jnc.13842.

Age-dependent alterations to paraventricular nucleus insulin-like growth factor 1 receptor (IGF-1R) as a possible link between sympathoexcitation and inflammation

Olalekan M. Ogundele[1], **Charles C. Lee**[1], and **Joseph Francis**[1]

[1]Department of Comparative Biomedical Sciences, Louisiana State University School of Veterinary Medicine, Baton Rouge, Louisiana

Abstract

Modifications to neural circuits of the paraventricular hypothalamic nucleus (PVN) have been implicated in sympathoexcitation and systemic cardiovascular dysfunction. However, to date, the role of insulin-like growth factor 1 receptor (IGF-1R) expression on PVN pathophysiology is unknown. Using confocal immunofluorescence quantification and electrophysiological recordings from acute PVN slices, we investigated the mechanism through which age-dependent IGF-1R depletion contributes to the progression of inflammation and sympathoexcitation in the PVN of spontaneously hypertensive rats (SHR). Four and twenty weeks old SHR and Wistar Kyoto (WKY) rats were used for this study. Our data showed that Angiotensin I/II and pro-inflammatory high mobility box group protein 1 (HMGB1) exhibited increased expression in the PVN of SHR versus WKY at 4 weeks ($p<0.01$), and were even more highly expressed with age in SHR ($p<0.001$). This correlated with a significant decrease in IGF-1R expression, with age, in the PVN of SHR when compared with WKY ($p<0.001$) and were accompanied by related changes in astrocytes and microglia. In subsequent analyses, we found an age-dependent change in the expression of proteins associated with IGF-1R signaling pathways involved in inflammatory responses and synaptic function in the PVN. MAPK/ErK was more highly expressed in the PVN of SHR by the 4th week ($p<0.001$; vs WKY), while expression of neuronal nitric oxide synthase (nNOS; $p<0.001$) and calcium-calmodulin dependent kinase II alpha (CamKIIα; $p<0.001$) were significantly decreased by the 4th and 20th week respectively.

Age-dependent changes in MAPK/ErK expression in the PVN correlated with an increase in the expression of vesicular glutamate transporter (VGLUT2) ($p<0.001$ vs WKY), while decreased levels of CamKIIα was associated with a decreased expression of tyrosine hydroxylase ($p<0.001$) by the 20th week. In addition, reduced labeling for GABA in the PVN of SHR ($p<0.001$) correlated with a decrease in nNOS labeling ($p<0.001$) when compared with the WKY by the 20th week. Electrophysiological recordings from neurons in acute slice preparations of the PVN of 4 weeks old SHR revealed spontaneous post-synaptic currents of higher frequency when compared with neurons from WKY PNV slices of the same age ($p<0.001$; $n=14$ cells). This also correlated

Corresponding Author: Joseph Francis [jfrancis@lsu.edu Tel: 225-578-9414].

Footnote: depletion, decline and decrease were used interchangeably in the manuscript. This basically implies a decrease or reduction in labeling. Up-regulation, over-expression and increase were also used interchangeably to denote an increase in labeling.

Competing interests: The author states that the present manuscript presents no conflict of interest.

with an increase in post-synaptic densities (PSD-95) in the PVN of SHR when compared with the WKY ($p<0.001$). Overall, we found an age-dependent reduction of IGF-1R, and related altered expression of associated downstream signaling molecules that may represent a link between the concurrent progression of synaptic dysfunction and inflammation in the PVN of SHR.

Keywords

IGF-1/IGF-1R; Angiotensin II; SHR; PVN; Sympathoexcitation; EPSCs

Introduction

Dysregulation of synaptic function in the neural cardiovascular control center has been implicated in the cause and progression of hypertension (Shell et al., 2016; Suyama et al., 2015; Glass et al., 2015). Projections from the paraventricular hypothalamic nuclei (PVN) to the nucleus of solitary tract (NTS) and rostral ventrolateral medulla (RVLM) constitutes the pre-autonomic sympathetic system which in turn projects to the intermediolateral grey column (IML) to reach the cardiac sympathetic plexus (Pyner, 2014; Affleck et al., 2012). This circuit has also been implicated in the neural control of metabolism, electrolyte and fluid balance through the regulation of neuropeptides, such as Angiotensin II, Orexin and adiponectin, and neurotransmitters involved in hypothalamic-hypophysial homeostatic regulation (Eliava et al., 2016; Foppen et al., 2016; Hao et al., 2016).

Aging-related changes in the brain are often associated with increased expression of pro-inflammatory cytokines, oxidative stress and synaptic changes that contributes to the observed pathophysiology in neural systems (Badowska-Szalewska. et al., 2015; Gupta et al., 2014). Furthermore, hypertension has been described as an inflammatory disorder associated with elevated levels of circulating Angiotensin II (Ang II) and pro-inflammatory cytokines that alters synaptic activity (Takesue et al., 2016a; Hay, 2016; Qi et al., 2015). Ang II activates Angiotensin type 1 Receptor (AT_1R) which increases oxidative stress and inflammation through up regulation of NADPH Oxidase (NOX) and depletion of neuronal nitric oxide synthase (nNOS) (Topchiy et al., 2013; Yuan et al., 2015).

Ang II-induced inflammation is also associated with an increase in cytoplasmic translocation of high mobility group box protein 1 (HMGB1), known to promote danger associated molecular pattern signaling (DAMP) (Song et al., 2014; Nair et al., 2015; Enokido et al., 2008; Qi et al., 2015). Synergistically, Ang II and HMGB1 facilitate the depletion of nNOS and adversely alter synaptic activity (Reis et al., 2016). Owing to its effect on nNOS, Ang II can reduce the bioavailability of NO and inhibitory GABA neurotransmission while increasing paraventricular sympathoexcitation in hypertension (Yuan et al., 2015; Wu et al., 2016; Jang et al., 2105; Campese et al., 2002; Li and Pan, 2005; Zhang t al., 1998; DiCarlo et al., 2002). Similarly, an increase in circulating Ang II, in hypertension, has been linked to the upregulation of downstream molecules and receptors implicated in HMGB1-driven inflammation and synaptic dysfunction (Song et al., 2014; de Kloet et al., 2013; Dange et al., 2015; Lin et al., 2015). HMGB1 signaling may alter the synaptic activity of catecholamines by activating toll-like receptor 4 (TLR4) and downstream molecules, like NF-κB: which

favour the transcription of genes known to promote tyrosine hydroxylase synthesis (Kizaki et al., 2009; Liu et al., 2014; Lin et al., 1995; Zhang et al., 2015; Abdelsalam and Safar, 2015). In a related pathway, Ang II-mediated activation of *MAPK/ErK1/ErK2* is also associated with the modulation of inflammation, and increased vesicular release of presynaptic glutamate in the brain (Tao et al., 2016; Yu et al., 2016; Zucker and Gao, 2005; Park and Rongo, 2016; Zhou et al., 2016). Thus, Ang II-induced sympathoexcitation, in the PVN, may involve the alteration of excitatory (glutamate and cathecolamines) and inhibitory (GABA) systems through signaling molecules generated in the inflammatory pathways (Dendorfer et al., 2002; Liu et al., 2014).

Insulin-like growth factor 1 receptor (IGF-1R) is also involved in the regulation of synaptic activity and attenuation of inflammation in the nervous system (Zhao et al., 1997; Sernia et al., 1997). IGF-1R is relatively abundant in post-synaptic terminals where it influences synaptic plasticity through the regulation of catecholaminergic β_2 and ionotropic glutamate receptors (Chesik et al., 2008; Fernandez and Torres-Alemán, 2012; Ding et al., 2006). In addition to its effects on synaptic function, IGF-1R promotes the release of calcium-calmodulin dependent kinase II (CamKIIα), which attenuates inflammation by inactivating molecules involved in HMGB1-dependent DAMP signaling (Ding et al., 2006; Sinha et al., 2011). Furthermore, cross-talk between IGF-1 and Ang II signaling pathways is possible; especially in the alteration of receptor expression patterns involving ErK1/ErK2 signaling downstream of Ang II receptor (AT_1R) and IGF-1R (Jia et al., 2011). However, to date, the role of IGF-1R expression patterns in the PVN of SHR, and its possible role in inflammation and sympathoexcitation has yet to be elucidated. Thus, we investigated age-related changes in IGF-1R/Ang II signaling relative to the concurrent progression of inflammation and sympathoexcitation in the PVN of SHR.

Methods

Animal Preparation

Spontaneously hypertensive rats (SHR) and Wistar Kyoto Rats (WKY) were procured from the Charles River Laboratory (Wilmington, WA). Four (4)- and 20-week old male rats were separated into four groups of *n=10* animals each and maintained under standard laboratory condition. All animal handling procedures were done using guidelines approved by the Institutional Animal Care and Use Committee (IACUC) of the Louisiana State University.

Immunohistochemistry

Rats were perfused transcardially with 10mM PBS (pH 7.4). Subsequently, the perfusion fluid was replaced by 4% phosphate buffered paraformaldehyde (4% PFA). The whole brain was removed and fixed in 4% PFA for 24 hours following which the tissue was cryopreserved in 4% PFA containing 30% Sucrose (4°C). Free-floating cryostat sections (40μm) were obtained and washed (3 times) in 10mM PBS (pH 7.4). In order to block non-specific protein interaction, sections were incubated in normal goat or rabbit serum, respectively (Vector Labs, Burlingame, CA) prepared in 10mM PBS (with 0.03% Triton-X 100) at room temperature for 2h. Sections were washed three times in PBS and incubated in a primary antibody solution overnight at 4°C. Primary antibodies [Goat Anti-Ang I/II (1:

250; Santa Cruz-sc-7419, Dallas, TX), Rabbit anti-IGF-1R (1:100; ThermoScientific-MA5-15148, Waltham, MA), Rabbit anti-HMGB1 (1:300; Abcam-ab79823, Cambridge, UK), Rabbit anti-Tyrosine Hydroxylase (1:500; Abcam-ab6211), Rabbit anti-GABA (1:200; Abcam-ab8891), Rabbit anti-nNOS (1:200; Cell Signaling-#4231, Danvers, MA), Rabbit anti-MAPK/ErK1/ErK2 (1:100; Cell Signaling-#9102), Mouse anti-CamKIIα (1:100; Cell Signaling-#50049), Rabbit anti-PSD-95 (1:100; Cell Signaling-#2507), Guinea pig anti-VGLUT 2 (1:250; EMD Millipore-AB2251, Danvers, MA), Mouse anti CD11b (1:250; Abcam-AB1211), Rabbit anti GFAP (1:300; Abcam-AB7620), and Rabbit anti NeuN-Alexa 488 Conjugate (Abcam; 1:300)] were prepared in 10mM PBS, 0.03% Triton X-100 and normal goat or rabbit serum. Further processing involved incubation in secondary antibody solution [Goat anti-Rabbit Alexa-568, Goat anti-Rabbit Alexa-594, Goat anti-Mouse Alexa-568, Rabbit anti-Goat Alexa 594, Goat anti-Guinea Pig Alexa 568 (Thermofisher; 1:1000), 10mM PBS, 0.03% Triton X-100 and normal serum] for 1h at room temperature in a dark enclosure. Immunolabeled sections were washed and mounted on gelatin-coated slides with plain anti-fade mounting medium or mountant containing DAPI (Vector Labs).

Confocal Microscopy and Quantification

The distribution of proteins, receptors and enzymes were imaged using immunofluorescence quantification and confocal microscopy on an Olympus FluoView 10i (Olympus America, Center Valley, PA). Cell and protein counting was done using Image J (NIH, Betheda, MD) and compared for the four groups in *One Way ANOVA* with Tukey post-hoc test (GraphPad Prism Version 5). Statistical significance set at $P<0.05$ (95% Confidence Interval). The outcome was presented in a grouped bar chart with error bars; representing the mean and standard error of mean respectively (mean±SEM).

Electrophysiology

In separate slice electrophysiological experiments, 4 weeks old SHR and WKY rats were decapitated after deep sedation with isoflurane. The whole brain was dissected and kept in ice-cold oxygenated artificial cerebrospinal fluid [ACSF; in mM 125 NaCl, 25 $NaHCO_3$, 3 KCl, 1.25 NaH_2PO_4, 1 $MgCl_2$, 2 $CaCl_2$ and 25 Glucose]. Coronal slices (500μm thick) containing the PVN were obtained in cold oxygenated ACSF using a vibrotome and were immediately transferred into an oxygenated ACSF bath maintained at 34°C. After a recovery period of 1h, the brain slices were transferred to a perfusion chamber mounted on an Olympus BX 51 Microscope (Olympus America). Flame pulled low resistance glass pipette electrode (3-5 MΩ) were prepared on a Flaming/Brown P-97 Micropipette puller (Stutter Instruments, Novato, CA) and filled with an intracellular solution [in mM 135 Potassium gluconate, 7 NaCl, 10 4-(2hydroxy ethyl)-1-piperazineethanesulfonic gluconate, 1-2 Na_2ATP, 0.3 Guanosine Trisphosphate (GTP) and $MgCl_2$; the pH was adjusted with KOH and final Osmolality was set at 290mOsm]. Using a micromanipulator, the electrode was visually guided to create a loose patch in order to isolate post-synaptic currents (PSC) (n=9 cells in SHR and n=5 cells in WKY) in voltage clamp mode (Leech and Holz, 1994). Spontaneously evoked activity and changes in membrane potential were detected using Multiclamp 700B Amplifier and Digidata 1440A digital acquisition system (Molecular Devices, Sunnyvale, CA) with filters set at 1KHz and 10Hz (upper and lower band pass).

Pipette access resistance ranged from 5-20MΩ throughout the duration of the recording. Spontaneously evoked PSCs were measured with voltage held (V_h) at $-60mV$ with no agonists added to the bath ASCF for SHR and WKY cortical slices. Analysis of recordings was performed in ClampFit (Molecular Devices).

Results

Ang II

At 4 weeks, the expression of Ang I/II was higher in SHR compared to WKY ($P<0.01$). Ang I/II expression was significantly increased with age in the PVN of $SHR^{20weeks}$ compared with SHR^{4weeks} ($p<0.001$). Similarly, the expression of Ang I/II in the PVN increased with age in the WKY ($p<0.05$) (Fig. 1A-B). At higher magnification, Ang I/II was mostly localized within the cytoplasm and interneuronal spaces in the PVN of SHR. By contrast, the WKY PVN neurons expressed Ang I/II predominantly in the interneuronal space (Fig. 1C) by the 4^{th} week. Ang I/II over-expression was observed both intracellularly and in the extra-neuronal compartments within the PVN of $SHR^{20weeks}$ (Fig. 1C; $p<0.01$).

HMGB1

No significant change occurred in HMGB1 expression in the PVN when the SHR was compared with the WKY by the 4^{th} week. However, for both groups, by the 20^{th} week, nuclear HMGB1 expression increased significantly (Fig. 2; $p<0.001$). No significant difference in HMGB1 expression was observed in the PVN of SHR and WKY by the 20^{th} week (Fig.2A-B), however, further analysis showed predominantly extra nuclear HMGB1 in the PVN of SHR (Fig. 2C).

CD11b and GFAP

At 4 weeks, the SHR showed a lower count for microglia when compared with the WKY (Fig. 3A-B; $p<0.05$). Furthermore, distribution of microglia increased in the PVN of SHR ($p<0.001$), but not WKY, by the 20^{th} week. However, the microglia field area was 20% wider in the SHR when compared with the WKY by the 4^{th} and 20^{th} week (Fig. 3C-D; $p<0.01$and $p<0.05$). In subsequent analysis, we evaluated the distribution of astrocytes and found a prominent increase in population in the PVN of SHR - versus the WKY - at 4 weeks ($p<0.001$). No significant change in astrocyte count was seen in the PVN of SHR at 20 weeks when compared with the WKY rats (Fig. 3E-F). Similar to our observations for microglia, astrocytes found in the PVN of SHR showed a prominent increase in astrocytic field by the 4^{th} and 20^{th} week when compared with the WKY (Fig. 3G-H; $p<0.001$ and $p<0.001$ respectively).

IGF-1R

Analysis of double-labeled (NeuN and IGF-1R) sections showed that IGF-1R was preferentially expressed in the PVN, when compared with adjacent thalamic and ventral hypothalamic areas (Fig. 4A-B). This suggests that IGF-1R is particularly important for PVN function and changes in the expression of IGF-1R in the PVN may contribute to inflammatory response and synaptic dysfunction in SHR. By the 4^{th} week, no significant change was seen in IGF-1R expression in the PVN when the SHR was compared with WKY.

However, IGF-1R reduced with age when $SHR^{20weeks}$ was compared with SHR^{4weeks} ($p<0.001$). Similarly, a decline in IGF-1R, with age, was observed in the WKY ($p<0.05$). It is noteworthy to mention that IGF-1R expression was empirically higher in the WKY versus the SHR of the same age (20 weeks) (Fig. 4C-D).

Downstream molecules of IGF-1R signaling in the PVN of SHR

Previous studies have shown, extensively, the role of IGF-1R signaling in the development and maintenance of synapses in the brain. Furthermore, the progression of neural hypertension has been shown to involve synaptic dysregulation in the PVN. In addition to the observed age-related loss of IGF-1R in the PVN (versus WKY; Fig. 4), we evaluated the expression pattern of proteins (CamKIIα, MAPK/ErK1/ErK2) involved in IGF-1R signaling, synaptic function and inflammation.

Our data showed that CamKIIα expression did not change significantly in the PVN of SHR when compared with WKY at 4 weeks. However, CamKIIα expression was significantly lower by the 20th week compared to SHR^{4weeks} ($p<0.001$) (Fig. 4E-F *CamKIIα*). By contrast, WKY showed no significant change in CamKIIα expression with age, and had higher expression than the SHR by the 20^{th} week ($p<0.001$).

MAPK/ErK was upregulated in the PVN of SHR by the 4^{th} week when compared with WKY ($p<0.001$). Since MAPK/ErK has been implicated in synaptic function and inflammation through the phosphorylation of CamKIIα, an upregulated MAPK/ErK may downregulate IGF-1R function through the inhibition of CamKIIα. Surprisingly, MAPK/ErK expression was reduced with age in SHR when SHR^{4weeks} was compared with $SHR^{20weeks}$ ($p<0.05$). Furthermore, $SHR^{20weeks}$ showed a significant decline in MAPK/ErK versus the WKY of same age (Fig. 4E-F *MAPK/ErK*).

In order to correlate the significance of MAPK/ErK/CamKIIα expression to the change in synaptic function and inflammation mediated through oxidative stress, we evaluated the distribution of nNOS in the PVN of SHR and WKY rats at 4 and 20 weeks. Interestingly, we observed no significant change in nNOS with age in the SHR and WKY rats (4 weeks versus 20 weeks). However, nNOS was significantly lower in the PVN of SHR at 4 and 20 weeks versus the WKY ($p<0.001$) (Fig. 4E-F *nNOS*). This outcome suggests a persistent level of oxidative stress between the 4^{th}-20^{th} week in the PVN of SHR. Furthermore, changes in nNOS have been shown to cause alterations in excitatory NMDAR and inhibitory GABA activity during inflammation and sympathoexcitation.

Neurotransmitter systems

In order to elucidate the role of age-related PVN inflammation on synaptic dysfunction, we evaluated the relationship between the secondary signaling molecules in IGF-1R/HMGB1 signaling pathways (CamKIIα, MAPK/ErK and nNOS) and the expression of excitatory (tyrosine hydroxylase, glutamate) and inhibitory (GABA) neurotransmitters molecules in the PVN of SHR and WKY. Our results showed an increase in tyrosine hydroxylase expression when SHR^{4weeks} was compared with $SHR^{20weeks}$ ($p<0.001$; Fig. 5A-C), which interestingly was also observed in the WKY ($p<0.01$). However, the SHR showed a more prominent increase at 20 weeks versus the WKY ($p<0.05$; Fig. 5A-C). Alterations in the expression of

MAPK/ErK were associated with increased presynaptic vesicular glutamate transporter (VGLUT 2) expression with age in the PVN of SHR when SHR^{4weeks} was compared with $SHR^{20weeks}$ ($p<0.001$; Fig. 6A-C). Similarly, VGLUT2 expression was higher in the PVN of the SHR when compared with the WKY by the 20^{th} week ($p<0.01$). From these findings, we suggest that depletion of IGF-1R in the PVN may be associated with the progression of sympathoexcitation through increased catecholaminergic and glutamatergic signaling events. Subsequently, we evaluated the significance of nNOS depletion in the PVN of SHR on the inhibitory GABAergic system. A significant reduction in GABA was observed in the PVN of both SHR and WKY when the 4^{th} week was compared with the 20^{th} week scores ($p<0.001$). However, the SHR showed a more significant decrease in GABA when compared with the WKY by the 20^{th} week ($p<0.05$; Fig. 7A-C).

Synaptic Modifications

Quantification and analysis of post-synaptic density (PSD-95) showed that changes in the expression of excitatory and inhibitory neurotransmitter systems were associated with postsynaptic morphological modifications in the PVN of SHR (Fig. 8A). At 4 weeks, the PSD-95 expression was higher in the SHR when compared with the WKY ($p<0.05$). However, by the 20^{th} week, a decline in PSD-95 was seen in the WKY ($p<0.05$) while the expression of the protein increased significantly in the SHR ($p<0.001$) (Fig. 8B-C).

Physiological changes

Subsequent characterization of physiological properties of PVN neurons using whole-cell patch clamp electrophysiology showed a defective baseline action potential for PVN neurons of SHR^{4weeks} versus the WKY in current clamp (Fig. 9A; $p<0.001$). In voltage clamp mode, the frequency of inward currents was significantly higher in SHR versus the WKY (mean ±SEM, $p<0.001$); although the amplitude was unchanged (Fig. 9A-B). The EPSCs were associated with abnormal phases of repetitive firing when the SHR was compared with the WKY (Fig. 9B). The frequency of spontaneously evoked currents was significantly higher in the SHR versus the WKY when the holding voltage (V_h) was set at −60mV. Furthermore, the amplitude of the spontaneous inward currents increased significantly in the PVN neurons of SHR; when compared with the WKY (Fig. 9B).

Discussion

Although Ang II-induced hypertension involves neural and systemic cardiovascular changes, this study focused exclusively on some of the neural PVN changes associated with the spontaneous development of sympathoexcitation in SHR and control WKY rats. Previous studies have shown that SHR become hypertensive after the fifth week and remain so until the end of life (end organ damage) when compared with the control WKY strain (Care et al., 2016; Kilick-Erkek et al., 2015; Lindesay et al., 2016; Gowrisankar and Clark, 2016). The role of Angiotensinergic activation in the PVN and systemic circulation has long been described in the cause and progression of hypertension in humans and rodent experimental models alike (Takesue et al., 2016; Shell et al., 2016). Furthermore, activation of AT_1R, by Ang II, in the PVN may contribute to the progression of neuroinflammation and sympathoexcitation described in SHR and other hypertensive models (Ogawa et al., 2012;

Kishi, 2016). However, the mechanism through which sympathoexcitation and inflammation progresses simultaneously in the PVN to create the hypertensive state has yet to be elucidated.

IGF-1R signaling activates *CamKIIα* which interacts structurally with dopaminergic D2 receptor (D2R) and controls β_2R during catecholaminergic neurotransmission (Chesik et al., 2008; Kawaai et al., 2015). Through this mechanism, IGF-1R can indirectly regulate the synaptic activity of ionotropic glutamate receptors (*AMPAR* and *NMDAR*) by exerting control on calcium movement (Hoerndli et al., 2015; Kawaai et al., 2015; Chesik et al., 2008). However, during Ang II mediated inflammation in SHR, IGF-1R and its messenger molecule (CamKIIα) are down regulated and may result in the loss of catecholaminergic and glutamatergic synaptic control (Fig. 10). Furthermore, an increase in MAP/ErK signaling- as a result of IGF-1R/CamKIIα depletion - promotes the pre-synaptic release of glutamate (excitatory synaptic activity) (Yu et al., 2016). Taken together, the outcome of this study suggests that IGF-1R depletion with age may represent the hallmark of synaptic dysfunction and inflammation associated with early onset neural hypertension in SHR. This was in agreement with the reports by Zhao and co-workers (1997) that described an age-dependent change in IGF-1R as a factor involved in neuroinflammation.

IGF-1R signaling in Ang II-induced PVN Inflammation

We have shown that elevated PVN Ang I/II is associated with a decrease in IGF-1R and may represent a mechanism that promotes sympathoexcitation and inflammation in neural hypertension. From our observations, we hypothesize that an age-dependent IGF-1R depletion may be involved in the PVN pathophysiological characteristics of SHR and hypertension models (Fig.1–4). Based on these observations and studies by other groups (Takesue et al., 2016a; Yu et al., 2015), we deduce that an increase in PVN Ang II with age in SHR promotes inflammation by reducing neurotropin receptor expression (IGF-1R). This is consistent with the results of Okajima and Harada (2008) that describe a decline in serum IGF-1 in SHR (when compared with the WKY). Furthermore, treatment with IGF-1 through pharmacological stimulation of sensory neurons reduces the deleterious effects by blocking inflammation in SHR (Okajima and Harada, 2006).

The expression of pro-inflammatory cytokine (HMGB1), involved in the onset of DAMP signaling, increased with age in the PVN of SHR and WKY. However, in the PVN of SHR, cytoplasmic translocation (activation) of HMGB1 was more prominent when compared with the WKY by the 20^{th} week. Mechanistically, Ang II may facilitate neurotropin depletion through the activation of AT_1R, which increases MAPK/ErK signaling. MAPK/ErK increases JNK and *cJUN* which promotes nuclear activation and post-translational modifications of HMGB1 (Dange et al., 2015; Chen et al., 2012; Chen et al., 2012). In addition, previous studies have shown that an increase in MAPK/ErK is associated with up-regulated NOX and oxidative stress (Simões et al., 2015; Morales et al., 2014). As a result, nNOS and other antioxidant (induced nitric oxide synthase and Cyclooxygenase) systems are depleted leading to an increase in inflammation through oxidative stress (Dai et al., 2014; Zhang t al., 1998; DiCarlo et al., 2002).

Quantification of MAPK/ErK in the PVN showed that the protein was up-regulated in the SHR at 4 weeks compared with the WKY ($p<0.001$; Fig. 4E-F). An increase in MAPK/ErK was associated with an age-dependent decrease in IGF-1R and CamKIIα by the 20th week. To support these findings, previous studies have shown that IGF-1R and CamKIIα are involved in the attenuation of inflammation through the phosphorylation of MAPK/ErK1/Erk2 (Waldsee et al., 2014; Cassilhas et al., 2012). Furthermore, a decline in IGF-1R signaling may promote inflammation through the loss of signaling molecules involved in the attenuation of inflammation (Lewis and Spandau, 2008). Based on these prepositions, we have shown that the PVN of SHR is characterized by an age-dependent decrease in IGF-1R/CamKIIα/nNOS and an increase in Ang II/HMGB1/MAPK/ErK.

Microglia and astrocytic activation in the PVN of SHR

A more aggressive progression of inflammation in the PVN of SHR was further supported by quantification data from microglia (CD11b) and astrocytic (GFAP) activation. As such, by the 4th week, depletion in *nNOS* was accompanied by an increase in astrocyte count, and astrocytic and microglia area fields when compared with the WKY (Fig. 3). Similar to our observations in this study, previous reports have shown that an increase in microglia (Dworak et al., 2012) or astrocytes (Thaler et al., 2012; Hsuchou et al., 2009) in the brain may contribute to the progression of sympathoexcitation in pre-autonomic sympathetic centers. Additionally, strong evidence suggests that early onset oxidative stress in the PVN of SHR involves the concurrent depletion of nNOS and astrocytic activation. As shown previously by Mandell and VandenBerg (1999), an upregulated MAPK/ErK pathway represents a common promoter of astrogliosis and oxidative stress during brain inflammation. Furthermore, active calcium signaling events has been identified in astrocytes during glutamatergic excitotoxicity and cell death (Ranaivo et al., 2012). Ultimately, these imply a critical role for astrocytic activation in the early onset of synaptic dysfunction seen in the SHR; especially, with respect to increased glutamatergic and catecholaminergic activity (Fig. 5–6). Although no significant increase was seen in microglia count, the morphology of the CD11b positive cells and field are suggestive of the onset of inflammatory response and DAMP signaling events. Evidently, a recent study has shown a strong relationship between upregulated microglia and neurons involved in the control of cardiovascular function (Kapoor et al., 2016). Accordingly, the data from Takesue and co-workers showed that both Ang II infusion model and SHR showed an increase in microglia activation in the PVN, and was associated with an elevated blood pressure; probably through sympathoexcitation (Takesue et al., 2016a, b).

IGF-1R signaling in inflammation and synaptic regulation

IGF-1R has been implicated in inflammation and synaptic function (Zhao et al., 1997). In this study, we identified proteins that act downstream of IGF-1R that are also involved in Ang II signaling and synaptic function. Based on this premise, we hypothesized that a change in the expression of IGF-1R may affect synaptic function and inflammation, in part, by altering the proteins in Ang II signaling pathway (Fig. 4). Primarily, we investigated Ang II-mediated inflammation involving the upregulation of HMGB1 in the PVN (Song et al., 2016), activation of MAPK/ErK and reduction of nNOS. Furthermore, elevated MAPK/ErK

has been implicated in the inactivation (phosphorylation) of CamKIIα and IGF-1R signaling (Yu et al., 2016; Zhao et al., 1997). Mechanistically, Ang II-mediated upregulation of MAPK/ErK, through HMGB1, facilitates an increase in VGLUT2 expression; associated with sympathoexcitation. Since IGF-1R and CamKIIα regulates the activity of catecholaminergic and ionotropic glutamate receptors (Chesik et al., 2008; Kawaai et al., 2015), MAPK/ErK-mediated change in CamKIIα may promote a change in catecholaminergic and glutamatergic neurotransmission. Furthermore, Ang II-related increase in MAPK/ErK is linked with the depletion of nNOS; associated with the inhibition of GABA (Reis et al., 2016).

Synaptic Modifications in the PVN

Neural projections from the PVN have been identified to the rostral ventrolateral medulla (RVLM) and represent the pre-autonomic sympathetic center that controls systemic cardiovascular function (Pyner, 2014; Shell et al., 2016). Excitatory glutamatergic and inhibitory GABA neuron populations have also been identified in parts of the PVN where they control the release of neuropeptides (Ang II), stress hormones (CRH) and electrolyte balance (Aguilera et al., 1995a; Aguilera et al., 1995b; Nillni, 2010). Thus, an increase in MAPK/ErK and a reduction in nNOS may alter excitatory and inhibitory neurotransmission, in the PVN, thus contributing to the progression of sympathoexcitation in systemic cardiovascular and metabolic disorders, similar to the reports by Yu et al. (2016) and others (Stratton et al., 2014; Tejas-Juárez et al., 2014; Kusek et al., 2013).

The PVN was thought to be a heterogeneous structure which contains several neurotransmitter systems that forms part of the descending hypothalamic hypophysial tract involved in neuroendocrine function (Holsen et al, 2013; Wamsteeker et al., 2013). Predominantly, the excitatory catecholaminergic system projects to the C1 catecholaminergic neuron population of the RVLM and increases the heart rate when activated (Badoer, 2001; Kishi et al., 2001). Similarly, pharmacological blockade of catecholaminergic receptors or degeneration of tyrosine hydroxylase positive neuron population in the PVN disrupts metabolism and heart rate (Zheng et al., 2014).

An increase in PVN Ang II can increase the threshold of sympathoexcitatory potentials and inflammation in the pre-autonomic sympathetic centers (PVN and RVLM), which often leads to hypertension (Kang et al., 2014; Glass et al., 2015; Garbor and Leenen, 2012). In this study, we compared the expression of excitatory (glutamate and catecholamine) and inhibitory (GABA) neurotransmitter system molecules in the PVN relative to inflammation and synaptic dysfunction. Our results showed that catecholaminergic and glutamatergic expression increased with age in the SHR versus WKY (Fig. 5–6), while GABA reduced profoundly in the SHR (Fig. 7). Similarly, structural modifications were observed in post-synaptic density morphology with age when the SHR was compared with WKY (Fig. 8). From these findings, we deduced that an increase in excitatory activity coupled with a decrease in inhibitory activity contributes to the progression of sympathoexcitation, with age, in the PVN. In slice physiological recordings from PVN neurons, spontaneously evoked PSCs were characteristic of the PVN neurons in SHR by the 4^{th} week. Interestingly, a study by Li et al. (2008) has shown similar synaptic dysfunction in the parasympathetic neurons of

SHR between the 11th and the 13th week. Although, synaptic dysregulation has been identified in adult SHR (Li et al., 2008), our findings here suggest it is an early event associated with upregulated MAPK/ErK and reduced nNOS expression; which may promote glutamatergic and reduce GABA activity respectively (Fig. 10).

Conclusion

Our findings indicate that IGF-1R is generally over expressed in the PVN, compared to the surrounding hypothalamus, and reduced more prominently with age in the SHR. We have shown that an increase in MAPK/ErK and decrease in nNOS were characteristic of the PVN in SHR by the 4th week; when compared with the WKY. In addition, the PVN neurons, at this time showed abnormal EPSCs attributable to synaptic dysfunction. By the 20th week, imbalance between excitatory (glutamate/cathecolamines) and inhibitory (GABA) neurotransmitter systems was accompanied by an increase in pro-inflammatory cytokines, depletion of IGF-1R and synaptic regulator (CamKIIα). Taken together, an age-dependent change in the expression pattern of proteins involved in the synaptic and inflammatory pathways of IGF-1R was linked with the progression of synaptic dysfunction and inflammation in the PVN of SHR.

Acknowledgments

This study was supported by the IBRO-ISN Fellowship 2014 awarded to OOM. NIH Grant R03 MH 104851 and Louisiana Board of Regents RCS Grant RD-A-09 awarded to CCL. SVM CORP Funds awarded to JF.

References

1. Abdelsalam RM, Safar MM. Neuroprotective effects of vildagliptin in rat rotenone Parkinson's disease model: role of RAGE-NFκB and Nrf2-antioxidant signaling pathways. J Neurochem. 2015 Jun; 133(5):700–7. (2015). [PubMed: 25752913]
2. Affleck VS, Coote JH, Pyner S. The projection and synaptic organisation of NTS afferent connections with presympathetic neurons, GABA and nNOS neurons in the paraventricular nucleus of the hypothalamus. Neuroscience. 2012 Sep 6.219:48–61. (2012). [PubMed: 22698695]
3. Aguilera G, Kiss A, Luo X. Increased expression of type 1 angiotensin II receptors in the hypothalamic paraventricular nucleus following stress and glucocorticoid administration. J Neuroendocrinol. 1995 Oct; 7(10):775–83. (1995). [PubMed: 8563720]
4. Aguilera G, Young WS, Kiss A, Bathia A. Direct regulation of hypothalamic corticotropin-releasing-hormone neurons by angiotensin II. Neuroendocrinology. 1995 Apr; 61(4):437–44. (1995). [PubMed: 7783857]
5. Badoer E. Hypothalamic paraventricular nucleus and cardiovascular regulation. Clin Exp Pharmacol Physiol. 2001 Jan-Feb;28(1–2):95–9. (2001). [PubMed: 11153547]
6. Badowska-Szalewska E, Krawczyk R, Ludkiewicz B, Moryś J. The effect of mild stress stimulation on the nerve growth factor (NGF) and tyrosine kinase receptor A (TrkA) immunoreactivity in the paraventricular nucleus (PVN) of the hypothalamus and hippocampus in aged vs. adult rats. Neuroscience. 2015 Apr 2.290:346–56. (2015). [PubMed: 25644424]
7. Campese VM, Ye S, Zhong H. Downregulation of neuronal nitric oxide synthase and interleukin-1beta mediates angiotensin II-dependent stimulation of sympathetic nerve activity. Hypertension. 2002 Feb; 39(2 Pt 2):519–24. (2002). [PubMed: 11882601]
8. Care AS, Sung MM, Panahi S, Gragasin FS, Dyck JR, Davidge ST, Bourque SL. Perinatal Resveratrol Supplementation to Spontaneously Hypertensive Rat Dams Mitigates the Development of Hypertension in Adult Offspring. Hypertension. 2016 Feb 29. (2016) pii: HYPERTENSIONAHA.115.06793. [Epub ahead of print].

9. Cassilhas RC, Lee KS, Fernandes J, Oliveira MG, Tufik S, Meeusen R, de Mello MT. Spatial memory is improved by aerobic and resistance exercise through divergent molecular mechanisms. Neuroscience. 2012 Jan 27.202:309–17. (2012). DOI: 10.1016/j.neuroscience.2011.11.029 [PubMed: 22155655]
10. Chen J, Zhang J, Xu L, Xu C, Chen S, Yang J, Jiang H. Inhibition of neointimal hyperplasia in the rat carotid artery injury model by a HMGB1 inhibitor. Atherosclerosis. 2012 Oct; 224(2):332–9. (2012) Epub 2012 Jul 24. DOI: 10.1016/j.atherosclerosis.2012.07.020 [PubMed: 22857898]
11. Chen XL, Sun L, Guo F, Wang F, Liu S, Liang X, Wang RS, Wang YJ, Sun YX. High-mobility group box-1 induces proinflammatory cytokines production of Kupffer cells through TLRs-dependent signaling pathway after burn injury. PLoS One. 2012; 7(11):e50668. (2015) Epub 2012 Nov 27. doi: 10.1371/journal.pone.0050668 [PubMed: 23209806]
12. Chesik D, Wilczak N, De Keyser J. IGF-1 regulates cAMP levels in astrocytes through a beta2-adrenergic receptor-dependant mechanism. Int J Med Sci. 2008 Aug 6; 5(5):240–3. (2008). [PubMed: 18690292]
13. Dai ZK, Lin TC, Liou JC, Cheng KI, Chen JY, Chu LW, Chen IJ, Wu BN. Xanthine derivative KMUP-1 reduces inflammation and hyperalgesia in a bilateral chronic constriction injury model by suppressing MAPK and NFκB activation. Mol Pharm. 2014 May 5; 11(5):1621–31. (2014) Epub 2014 Apr 7. DOI: 10.1021/mp5000086 [PubMed: 24669856]
14. Dange RB, Agarwal D, Teruyama R, Francis J. Toll-like receptor 4 inhibition within the paraventricular nucleus attenuates blood pressure and inflammatory response in a genetic model of hypertension. J Neuroinflammation. 2015 Feb 18.12:31. (2015). [PubMed: 25879545]
15. de Kloet AD, Pati D, Wang L, Hiller H, Sumners C, Frazier CJ, Seeley RJ, Herman JP, Woods SC, Krause EG. Angiotensin type 1a receptors in the paraventricular nucleus of the hypothalamus protect against diet-induced obesity. J Neurosci. 2013 Mar 13; 33(11):4825–33. (2013). DOI: 10.1523/JNEUROSCI.3806-12.2013 [PubMed: 23486953]
16. Dendorfer A, Thornagel A, Raasch W, Grisk O, Tempel K, Dominiak P. Angiotensin II induces catecholamine release by direct ganglionic excitation. Hypertension. 2002 Sep; 40(3):348–54. (2002). [PubMed: 12215478]
17. DiCarlo SE, Zheng H, Collins HL, Rodenbaugh DW, Patel KP. Daily exercise normalizes the number of diaphorase (NOS) positive neurons in the hypothalamus of hypertensive rats. Brain research. 2002; 955(1):153–160. [PubMed: 12419531]
18. Ding Q, Vaynman S, Akhavan M, Ying Z, Gomez-Pinilla F. Insulin-like growth factor I interfaces with brain-derived neurotrophic factor-mediated synaptic plasticity to modulate aspects of exercise-induced cognitive function. Neuroscience. 2006 Jul 7; 140(3):823–33. (2006). [PubMed: 16650607]
19. Dworak M, Stebbing M, Kompa AR, Rana I, Krum H, Badoer E. Sustained activation of microglia in the hypothalamic PVN following myocardial infarction. Auton Neurosci. 2012 Aug 16; 169(2): 70–6. (2012) Epub 2012 May 15. DOI: 10.1016/j.autneu.2012.04.004 [PubMed: 22591793]
20. Eliava M, Melchior M, Knobloch-Bollmann HS, Wahis J, da Silva Gouveia M, Tang Y, Ciobanu AC, Triana Del Rio R, Roth LC, Althammer F, Chavant V, Goumon Y, Gruber T, Petit-Demoulière N, Busnelli M, Chini B, Tan LL, Mitre M, Froemke RC, Chao MV, Giese G, Sprengel R, Kuner R, Poisbeau P, Seeburg PH, Stoop R, Charlet A, Grinevich V. A New Population of Parvocellular Oxytocin Neurons Controlling Magnocellular Neuron Activity and Inflammatory Pain Processing. Neuron. 2016 Mar 2. (2016) pii: S0896-6273(16)00088-X.
21. Enokido Y, Yoshitake A, Ito H, Okazawa H. Age-dependent change of HMGB1 and DNA double-strand break accumulation in mouse brain. Biochem Biophys Res Commun. 2008 Nov 7; 376(1): 128–33. (2008). [PubMed: 18762169]
22. Fernandez AM, Torres-Alemán I. The many faces of insulin-like peptide signalling in the brain. Nat Rev Neurosci. 2012 Mar 20; 13(4):225–39. (2013). [PubMed: 22430016]
23. Foppen E, Tan AA, Ackermans MT, Fliers E, Kalsbeek A. Suprachiasmatic nucleus neuropeptides and their control of endogenous glucose production. J Neuroendocrinol. 2016 Jan 20. (2016). doi: 10.1111/jne.12365
24. Gabor A, Leenen FH. Central neuromodulatory pathways regulating sympathetic activity in hypertension. J Appl Physiol 1985. 2012 Oct 15; 113(8):1294–303. (1985) Epub 2012 Jul 5. Review. DOI: 10.1152/japplphysiol.00553.2012 [PubMed: 22773773]

25. Glass MJ, Wang G, Coleman CG, Chan J, Ogorodnik E, Van Kempen TA, Milner TA, Butler SD, Young CN, Davisson RL, Iadecola C, Pickel VM. NMDA Receptor Plasticity in the Hypothalamic Paraventricular Nucleus Contributes to the Elevated Blood Pressure Produced by Angiotensin II. J Neurosci. 2015 Jul 1; 35(26):9558–67. (2015). [PubMed: 26134639]
26. Gowrisankar YV, Clark MA. Angiotensin II Regulation of Angiotensin Converting Enzymes in Spontaneously Hypertensive Rat Primary Astrocyte Cultures. J Neurochem. 2016 Apr 17. (2016) [Epub ahead of print]. doi: 10.1111/jnc.13641
27. Gupta D, Morley JE. Hypothalamic-pituitary-adrenal (HPA) axis and aging. Compr Physiol. 2014 Oct; 4(4):1495–510. (2014). DOI: 10.1002/cphy.c130049 [PubMed: 25428852]
28. Hao H, Luan X, Guo F, Sun X, Gong Y, Xu L. Lateral hypothalamic area orexin-A influence the firing activity of gastric distension-sensitive neurons and gastric motility in rats. Neuropeptides. 2016 Feb 16. (2016) pii: S0143-4179(16)30008-7. 26919916.
29. Hay M. Sex, the brain and hypertension: brain oestrogen receptors and high blood pressure risk factors. Clin Sci (Lond). 2016 Jan; 130(1):9–18. (2016). DOI: 10.1042/CS20150654 [PubMed: 26621877]
30. Hoerndli FJ, Wang R, Mellem JE, Kallarackal A, Brockie PJ, Thacker C, Madsen DM, Maricq AV. Neuronal Activity and CaMKII Regulate Kinesin-Mediated Transport of Synaptic AMPARs. Neuron. 2015 Apr 22; 86(2):457–74. (2015). [PubMed: 25843407]
31. Holsen LM, Lancaster K, Klibanski A, Whitfield-Gabrieli S, Cherkerzian S, Buka S, Goldstein JM. HPA-axis hormone modulation of stress response circuitry activity in women with remitted major depression. Neuroscience. 2013 Oct 10.250:733–42. (2013) Epub 2013 Jul 25. DOI: 10.1016/j.neuroscience.2013.07.042 [PubMed: 23891965]
32. Hsuchou H, He Y, Kastin AJ, Tu H, Markadakis EN, Rogers RC, Fossier PB, Pan W. Obesity induces functional astrocytic leptin receptors in hypothalamus. Brain. 2009; 132:889–902. (2009). [PubMed: 19293246]
33. Jang JH, Chun JN, Godo S, Wu G, Shimokawa H, Jin CZ, Jeon JH, Kim SJ, Jin ZH, Zhang YH. ROS and endothelial nitric oxide synthase (eNOS)-dependent trafficking of angiotensin II type 2 receptor begets neuronal NOS in cardiac myocytes. Basic Res Cardiol. 2015 May.110(3):21. (2015). [PubMed: 25804308]
34. Jia G, Aggarwal A, Yohannes A, Gangahar DM, Agrawal DK. Cross-talk between angiotensin II and IGF-1-induced connexin 43 expression in human saphenous vein smooth muscle cells. J Cell Mol Med. 2011 Aug; 15(8):1695–702. (2011). DOI: 10.1111/j.1582-4934.2010.01161.x [PubMed: 20731749]
35. Kang YM, Yang Q, Yu XJ, Qi J, Zhang Y, Li HB, Su Q, Zhu GQ. Hypothalamic paraventricular nucleus activation contributes to neurohumoral excitation in rats with heart failure. Regen Med Res. 2014 Jan 8.2(1):2. (2014). doi: 10.1186/2050-490X-2-2 [PubMed: 25984330]
36. Kapoor K, Bhandare AM, Nedoboy PE, Mohammed S, Farnham MM, Pilowsky PM. Dynamic changes in the relationship of microglia to cardiovascular neurons in response to increases and decreases in blood pressure. Neuroscience. 2016 Aug 4.329:12–29. (2016) Epub 2016 May 4. DOI: 10.1016/j.neuroscience.2016.04.044 [PubMed: 27155147]
37. Kawaai K, Mizutani A, Shoji H, Ogawa N, Ebisui E, Kuroda Y, Wakana S, Miyakawa T, Hisatsune C, Mikoshiba K. IRBIT regulates CaMKIIα activity and contributes to catecholamine homeostasis through tyrosine hydroxylase phosphorylation. Proc Natl Acad Sci U S A. 2015 Apr 28; 112(17): 5515–20. (2015) Epub 2015 Apr 14. DOI: 10.1073/pnas.1503310112 [PubMed: 25922519]
38. Kilic-Erkek O, Mergen-Dalyanoglu M, Kilic-Toprak E, Ozkan S, Bor-Kucukatay M, Turgut S. Exercise training and detraining process affects plasma adiponectin level in healthy and spontaneously hypertensive rats. Bratisl Lek Listy. 2015; 116(12):741–5. (2015). [PubMed: 26924145]
39. Kishi T. Heart Failure as a Disruption of Dynamic Circulatory Homeostasis Mediated by the Brain. Int Heart J. 2016 Mar 11. (2016) [Epub ahead of print].
40. Kishi T, Hirooka Y, Sakai K, Shigematsu H, Shimokawa H, Takeshita A. Overexpression of eNOS in the RVLM causes hypotension and bradycardia via GABA release. Hypertension. 2001 Oct; 38(4):896–901. (2001). [PubMed: 11641305]

41. Kizaki T, Shirato K, Sakurai T, Ogasawara JE, Oh-ishi S, Matsuoka T, Izawa T, Imaizumi K, Haga S, Ohno H. Beta2-adrenergic receptor regulate Toll-like receptor 4-induced late-phase NF-kappaB activation. Mol Immunol. 2009 Mar; 46(6):1195–203. (2009) Epub 2009 Jan 22. DOI: 10.1016/j.molimm.2008.11.005 [PubMed: 19167076]
42. Kusek M, Tokarski K, Hess G. Repeated restraint stress enhances glutamatergic transmission in the paraventricular nucleus of the rat hypothalamus. J Physiol Pharmacol. 2013 Oct; 64(5):565–70. (2013). [PubMed: 24304570]
43. Leech AC, Holz GG. Application of Patch Clamp Methods to the Study of Calcium Currents and Calcium Channels. Methods Cell Biol. 1994; 40:135–151. (1994). [PubMed: 8201974]
44. Lewis DA, Spandau DF. UVB-induced activation of NF-kappaB is regulated by the IGF-1R and dependent on p38 MAPK. J Invest Dermatol. 2008 Apr; 128(4):1022–9. (2008). [PubMed: 18059487]
45. Li DP, Pan HL. Angiotensin II attenuates synaptic GABA release and excites paraventricular-rostral ventrolateral medulla output neurons. J Pharmacol Exp Ther. 2005 Jun; 313(3):1035–45. (2005). [PubMed: 15681656]
46. Li DP, Yang Q, Pan HM, Pan HL. Pre- and postsynaptic plasticity underlying augmented glutamatergic inputs to hypothalamic presympathetic neurons in spontaneously hypertensive rats. Physiol. 2008 Mar 15; 586(6):1637–47. (2008) Epub 2008 Jan 31. DOI: 10.1113/jphysiol.2007.149732
47. Lin YZ, Yao SY, Veach RA, Torgerson TR, Hawiger J. Inhibition of nuclear translocation of transcription factor NF-kappa B by a synthetic peptide containing a cell membrane-permeable motif and nuclear localization sequence. J Biol Chem. 1995 Jun 16; 270(24):14255–8. (1995). [PubMed: 7782278]
48. Lindesay G, Ragonnet C, Chimenti S, Villeneuve N, Vayssettes-Courchay C. Age and hypertension strongly induce aortic stiffening in rats at basal and matched blood pressure levels. Physiol Rep. 2016 May.4(10) (2016) pii: e12805. doi: 10.14814/phy2.12805
49. Liu J, Buisman-Pijlman F, Hutchinson MR. Toll-like receptor 4: innate immune regulator of neuroimmune and neuroendocrine interactions in stress and major depressive disorder. Front Neurosci. 2014 Sep 30.8:309. (2014) eCollection 2014. doi: 10.3389/fnins.2014.00309 [PubMed: 25324715]
50. Liu Q, Wang T, Yu H, Liu B, Jia R. Interaction between interleukin-1 beta and angiotensin II receptor 1 in hypothalamic paraventricular nucleus contributes to progression of heart failure. J Interferon Cytokine Res. 2014 Nov; 34(11):870–5. (2014). [PubMed: 24955935]
51. Mandell JW, VandenBerg SR. ERK/MAP kinase is chronically activated in human reactive astrocytes. Neuroreport. 1999 Nov 26; 10(17):3567–72. (1999). [PubMed: 10619645]
52. Morales MG, Abrigo J, Meneses C, Simon F, Cisternas F1, Rivera JC, Vazquez Y, Cabello-Verrugio C1. The Ang-(1–7)/Mas-1 axis attenuates the expression and signalling of TGF-β1 induced by AngII in mouse skeletal muscle. Clin Sci (Lond). 2014 Aug; 127(4):251–64. (2014). DOI: 10.1042/CS20130585 [PubMed: 24588264]
53. Nair AR, Ebenezer PJ, Saini Y, Francis J. Angiotensin II-induced hypertensive renal inflammation is mediated through HMGB1-TLR4 signaling in rat tubulo-epithelial cells. Exp Cell Res. 2015 Jul 15; 335(2):238–47. (2015) Epub 2015 May 29. DOI: 10.1016/j.yexcr.2015.05.011 [PubMed: 26033363]
54. Nillni EA. Regulation of the hypothalamic thyrotropin releasing hormone (TRH) neuron by neuronal and peripheral inputs. Front Neuroendocrinol. 2010 Apr; 31(2):134–56. (2010). [PubMed: 20074584]
55. Ogawa K, Hirooka Y, Kishi T, Sunagawa K. Brain AT1 receptor activates the sympathetic nervous system through toll-like receptor 4 in mice with heart failure. J Cardiovasc Pharmacol. 2011 Nov; 58(5):543–9. (2011). [PubMed: 21822148]
56. Okajima K, Harada N. Regulation of inflammatory responses by sensory neurons: molecular mechanism(s) and possible therapeutic applications. Curr Med Chem. 2006; 13(19):2241–51. (2006). [PubMed: 16918352]

57. Okajima K, Harada N. Promotion of insulin-like growth factor-I production by sensory neuron stimulation; molecular mechanism(s) and therapeutic implications. Curr Med Chem. 2008; 15(29): 3095–112. (2008). [PubMed: 19075656]
58. Park EC, Rongo C. The p38 MAP kinase pathway modulates the hypoxia response and glutamate receptor trafficking in aging neurons. Elife. 2016 Jan 5.:5. (2016) pii: e12010. doi: 10.7554/eLife.12010
59. Pyner S. The paraventricular nucleus and heart failure. Exp Physiol. 2014 Feb; 99(2):332–9. (2014). [PubMed: 24317407]
60. Qi J, Yu XJ, Shi XL, Gao HL, Yi QY, Tan H, Fan XY, Zhang Y, Song XA, Cui W, Liu JJ, Kang YM. NF-κB Blockade in Hypothalamic Paraventricular Nucleus Inhibits High-Salt-Induced Hypertension Through NLRP3 and Caspase-1. Cardiovasc Toxicol. 2015 Oct 5. (2015a).
61. Qi L, Sun X, Li FE, Zhu BS, Braun FK, Liu ZQ, Tang JL, Wu C, Xu F, Wang HH, Velasquez LA, Zhao K, Lei FR, Zhang JG, Shen YT, Zou JX, Meng HM, An GL, Yang L, Zhang XD. HMGB1 Promotes Mitochondrial Dysfunction-Triggered Striatal Neurodegeneration via Autophagy and Apoptosis Activation. PLoS One. 2015 Nov 13.10(11):e0142901. (2015b). [PubMed: 26565401]
62. Ralay Ranaivo H, Hodge JN, Choi N, Wainwright MS. Albumin induces upregulation of matrix metalloproteinase-9 in astrocytes via MAPK and reactive oxygen species-dependent pathways. J Neuroinflammation. 2012 Apr 16.9:68. (2012). doi: 10.1186/1742-2094-9-68 [PubMed: 22507553]
63. Reis WL, Biancardi VC, Zhou Y, Stern JE. A Functional Coupling between Carbon Monoxide and Nitric Oxide Contributes to Increased Vasopressin Neuronal Activity in Heart Failure rats. Endocrinology. 2016 Mar 16. (2016) en20151958. [Epub ahead of print].
64. Sernia C, Zeng T, Kerr D, Wyse B. Novel perspectives on pituitary and brain angiotensinogen. Front Neuroendocrinol. 1997 Apr; 18(2):174–208. (1997). [PubMed: 9101259]
65. Shell B, Faulk K, Cunningham JT. Neural Control of Blood Pressure in Chronic Intermittent Hypoxia. Curr Hypertens Rep. 2016 Mar.18(3):19. (2016). doi: 10.1007/s11906-016-0627-8 [PubMed: 26838032]
66. Simões MR, Aguado A, Fiorim J, Silveira EA, Azevedo BF3, Toscano CM, Zhenyukh O, Briones AM, Alonso MJ, Vassallo DV, Salaices M. MAPK pathway activation by chronic lead-exposure increases vascular reactivity through oxidative stress/cyclooxygenase-2-dependent pathways. Toxicol Appl Pharmacol. 2015 Mar 1; 283(2):127–38. (2015) Epub 2015 Jan 14. DOI: 10.1016/j.taap.2015.01.005 [PubMed: 25596430]
67. Sinha S1, Koul N, Dixit D, Sharma V, Sen E. IGF-1 induced HIF-1α-TLR9 cross talk regulates inflammatory responses in glioma. Cell Signal. 2011 Nov; 23(11):1869–75. (2011) Epub 2011 Jul 3. DOI: 10.1016/j.cellsig.2011.06.024 [PubMed: 21756999]
68. Song C, Santisteban M, Zubcevic J, Raizada M. Involvement of neuronal high mobility group box 1 (HMGB1) in Angiotensin II-mediated neuronal-microglial interaction. Abstract 202. Hypertension. 2014; 64:A202. (2014).
69. Stratton MS, Staros M, Budefeld T, Searcy BT, Nash C, Eitel C, Carbone D, Handa RJ, Majdic G, Tobet SAN. Embryonic GABA(B) receptor blockade alters cell migration, adult hypothalamic structure, and anxiety- and depression-like behaviors sex specifically in mice. PLoS One. 2014 Aug 27.9(8):e106015. (2014). [PubMed: 25162235]
70. Suyama S, Kodaira-Hirano M, Otgon-Uul Z, Ueta Y, Nakata M, Yada T. Fasted/fed states regulate postsynaptic hub protein DYNLL2 and glutamatergic transmission in oxytocin neurons in the hypothalamic paraventricular nucleus. Neuropeptides. 2015 Aug 28. (2015) pii: S0143-4179(15)00087-6. [Epub ahead of print]. doi: 10.1016/j.npep.2015.08.008
71. Takesue K, Kishi T, Hirooka Y. Hypothalamic Activated Microglia Augment Blood Pressure Elevation during Early Developing Phase of Hypertension in Stroke-prone Spontaneously Hypertensive Rats. The FASEB Journal. Apr.2016 30(1) (2016b) Supplement 1235.2.
72. Takesue K, Kishi T, Hirooka Y, Sunagawa K. Activation of microglia within paraventricular nucleus of hypothalamus is NOT involved in maintenance of established hypertension. J Cardiol. 2016 Feb 10. (2016a).
73. Tao L, Qiu Y, Fu X, Lin R, Lei C, Wang J, Lei B. Angiotensin-converting enzyme 2 activator diminazene aceturate prevents lipopolysaccharide-induced inflammation by inhibiting MAPK and

NF-κB pathways in human retinal pigment epithelium. J Neuroinflammation. 2016 Feb 9.13(1): 35. (2016). doi: 10.1186/s12974-016-0489-7 [PubMed: 26862037]

74. Tejas-Juárez JG, Cruz-Martínez AM, López-Alonso VE, García-Iglesias B, Mancilla-Díaz JM, Florán-Garduño B, Escartín-Pérez RE. Stimulation of dopamine D4 receptors in the paraventricular nucleus of the hypothalamus of male rats induces hyperphagia: involvement of glutamate. Physiol Behav. 2014 Jun 22.133:272–81. (2014). [PubMed: 24805978]
75. Thaler JP, Yi CX, Schur EA, Guyenet SJ, Hwang BH, Dietrich MO, Zhao X, Sarruf DA, Izgur V, Maravilla KR, Nguyen HT, Fischer JD, Matsen ME, Wisse BE, Morton GJ, Horvath TL, Baskin DG, Tschöp MH, Schwartz MW. Obesity is associated with hypothalamic injury in rodents and humans. J Clin Invest. 2012; 122:153–62. (2012). [PubMed: 22201683]
76. Topchiy E, Panzhinskiy E, Griffin WS, Barger SW, Das M, Zawada WM. Nox4-generated superoxide drives angiotensin II-induced neural stem cell proliferation. Dev Neurosci. 2013; 35(4): 293–305. (2013) Epub 2013 Jun 8. DOI: 10.1159/000350502 [PubMed: 23751520]
77. Waldsee R, Eftekhari S, Ahnstedt H, Johnson LE, Edvinsson L. CaMKII and MEK1/2 inhibition time-dependently modify inflammatory signaling in rat cerebral arteries during organ culture. J Neuroinflammation. 2014 May 16.11:90. (2014). doi: 10.1186/1742-2094-11-90 [PubMed: 24886705]
78. Wamsteeker Cusulin JI, Füzesi T, Watts AG, Bains JS. Characterization of corticotropin-releasing hormone neurons in the paraventricular nucleus of the hypothalamus of Crh-IRES-Cre mutant mice. PLoS One. 2013 May 28.8(5):e64943. (2013). [PubMed: 23724107]
79. Wu ZT, Ren CZ, Yang YH, Zhang RW, Sun JC, Wang YK, Su DF, Wang WZ. The PI3K signaling-mediated nitric oxide contributes to cardiovascular effects of angiotensin-(1–7) in the nucleus tractus solitarii of rats. Nitric Oxide. 2016 Jan 30.52:56–65. (2016). [PubMed: 26686278]
80. Yu XJ, Zhang DM, Jia LL, Qi J, Song XA, Tan H, Cui W, Chen W, Zhu GQ, Qin DN, Kang YM. Inhibition of NF-κB activity in the hypothalamic paraventricular nucleus attenuates hypertension and cardiac hypertrophy by modulating cytokines and attenuating oxidative stress. Toxicol Appl Pharmacol. 2015 May 1; 284(3):315–22. (2015) Epub 2015 Mar 7. DOI: 10.1016/j.taap.2015.02.023 [PubMed: 25759242]
81. Yu Y, Wei SG, Zhang ZH, Weiss RM, Felder RB. ERK1/2 MAPK Signaling in Hypothalamic Paraventricular Nucleus Contributes to Sympathetic Excitation in Rats with Heart Failure after Myocardial Infarction. Am J Physiol Heart Circ Physiol. 2016 Jan 22. (2016) ajpheart.00703.2015.
82. Yuan X, Guo X, Deng Y, Zhu D, Shang J, Liu H. Chronic intermittent hypoxia-induced neuronal apoptosis in the hippocampus is attenuated by telmisartan through suppression of iNOS/NO and inhibition of lipid peroxidation and inflammatory responses. Brain Res. 2015 Jan 30.1596:48–57. (2015) Epub 2014 Nov 24. DOI: 10.1016/j.brainres.2014.11.035 [PubMed: 25463026]
83. Zhang Y, Chen Y, Wu J, Manaenko A, Yang P, Tang J, Fu W, Zhang JH. Activation of Dopamine D2 Receptor Suppresses Neuroinflammation Through αB-Crystalline by Inhibition of NF-κB Nuclear Translocation in Experimental ICH Mice Model. Stroke. 2015 Sep; 46(9):2637–46. (2015) Epub 2015 Aug 6. DOI: 10.1161/STROKEAHA.115.009792 [PubMed: 26251254]
84. Zhang K, Zucker IH, Patel KP. Altered number of diaphorase (NOS) positive neurons in the hypothalamus of rats with heart failure. Brain research. 786(1):219–225. (1998).
85. Zhao H, Zhao X, Cao X, Wu G. Age-Dependent Neuroimmune Modulation of IGF-1R in the Traumatic Mice. Immun Ageing. 2012 May 28.9(1):12. (1997). [PubMed: 22640633]
86. Zheng H, Liu X, Li Y, Mishra PK, Patel KP. Attenuated dopaminergic tone in the paraventricular nucleus contributing to sympathoexcitation in rats with Type 2 diabetes. Am J Physiol Regul Integr Comp Physiol. 2014 Jan 15; 306(2):R138–48. (2014). DOI: 10.1152/ajpregu.00323.2013 [PubMed: 24305061]
87. Zhou C, Sun R, Zhuang S, Sun C, Jiang Y, Cui Y, Li S, Xiao Y, Du Y, Gu H, Liu Q. Metformin prevents cerebellar granule neurons against glutamate-induced neurotoxicity. Brain Res Bull. 2016 Mar.121:241–5. (2016) Epub 2016 Feb 11. DOI: 10.1016/j.brainresbull.2016.02.009 [PubMed: 26876755]
88. Zucker IH, Gao L. The regulation of sympathetic nerve activity by angiotensin II involves reactive oxygen species and MAPK. Circ Res. 2005 Oct 14; 97(8):737–9. (2005). [PubMed: 16224073]

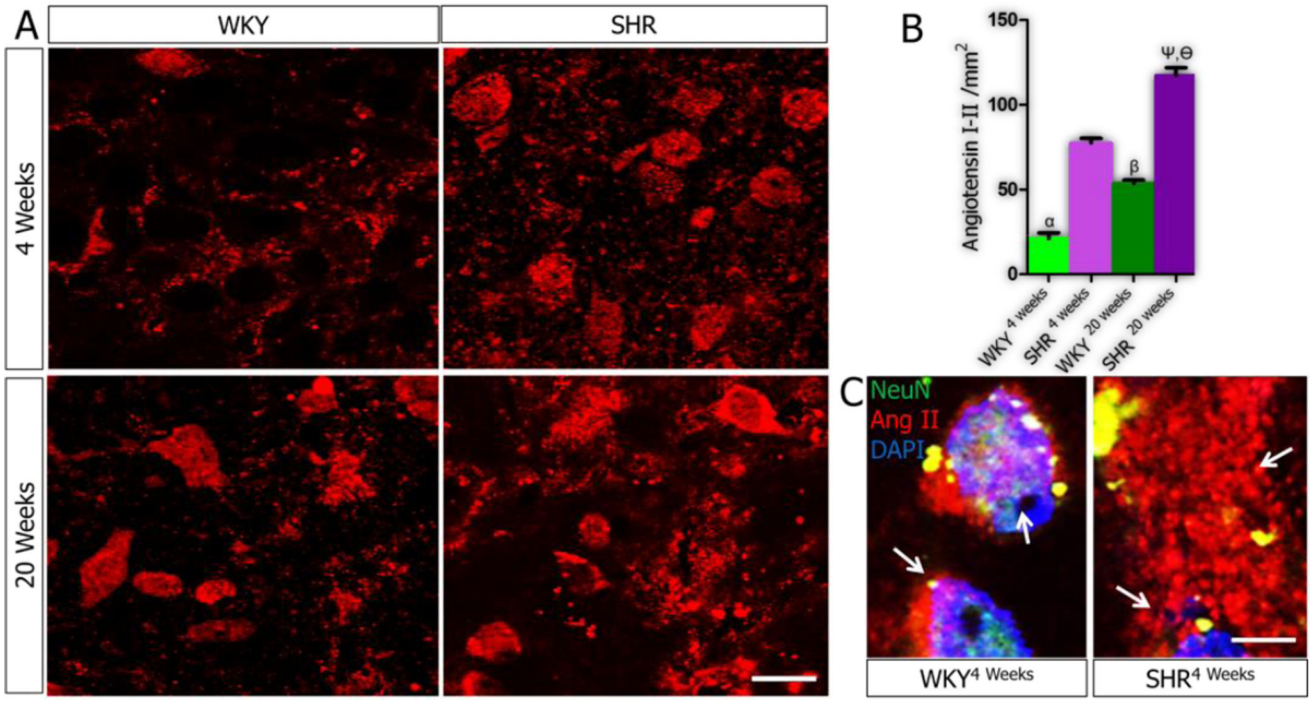

Figure 1.

A-C| Angiotensin I/II expression in the PVN. (**A**) Ang I/II was mostly localized within the interneuronal space of PVN neurons of WKY rats at 4 weeks (n=6, scale bar =20μm). By contrast, in the PVN of SHR^{4weeks}, Ang I/II increased in the PVN neurons and interneuronal space when compared with the WKY^{4weeks} (n=6, mean±SEM, $^{\alpha}p<0.01$). A slight increase in Ang I/II was observed in the PVN of the WKY at 20 weeks (n=6) when compared with the 4 weeks old rats (n=6, mean±SEM, $^{\beta}p<0.05$). The distribution of Ang I/II increased profoundly in the PVN of SHR when $SHR^{20weeks}$ was compared with the SHR^{4weeks} (n=6, mean±SEM, $^{\Psi}p<0.001$). Similarly, the distribution of Ang I/II was significantly higher in the SHR at 20 weeks, versus the WKY (n=6, mean±SEM, $^{\theta}p<0.001$). (**B**) Quantification of Ang I/II in the PVN of SHR and WKY at 4 and 20 weeks. (**C**) Higher magnification representative confocal images showing the localization Ang I/II in the cytoplasm and interneuronal spaces of PVN neurons (n=6, scale bar =5μm). The SHR showed a significantly higher Ang I/II expression in the neuron and interneuronal space when compared with the WKY (arrows).

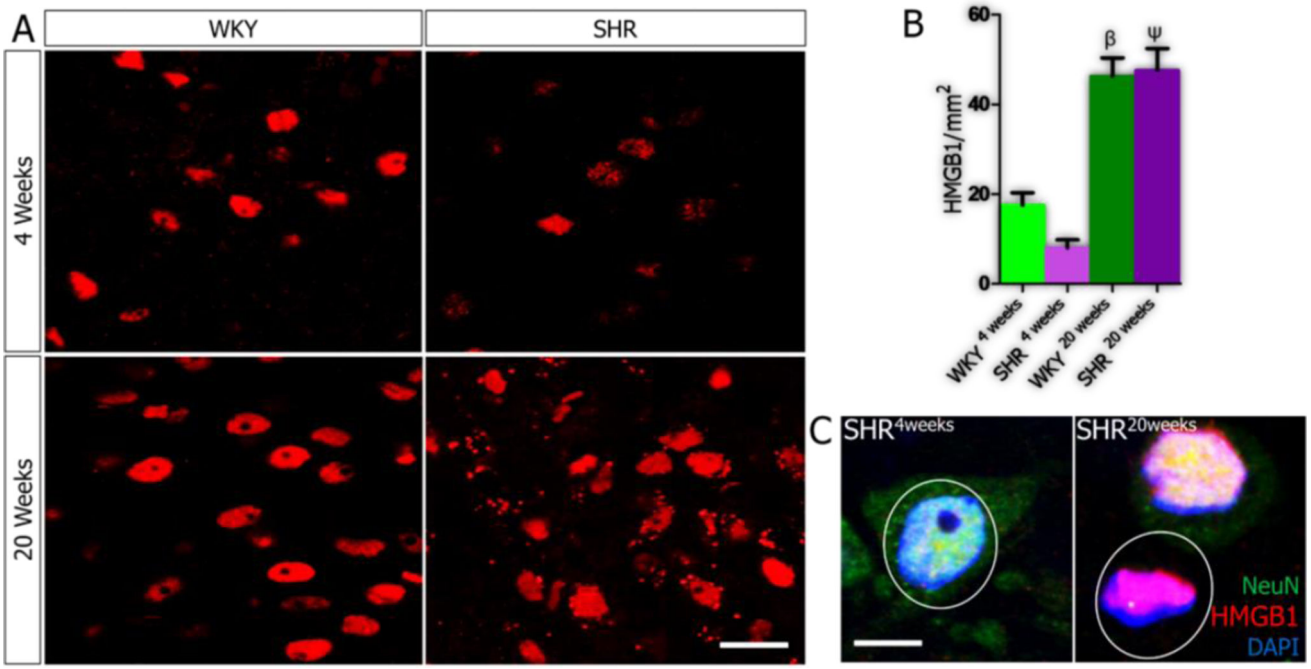

Figure 2.

A-C| Expression of HMGB1 in PVN of SHR and WKY rats. (**A**) No significant change was observed in the expression of HMGB1 when the SHR was compared with the WKY at 4 weeks (n=4). An increase in HMGB1 expression with age was seen in the WKY when the WKY^{4weeks} was compared with $WKY^{20weeks}$ (n=4, mean±SEM, $^{\beta}p<0.001$). Similarly, the distribution of HMGB1 in the nucleus of PVN neurons increased in SHR by the 20^{th} week; versus SHR^{4weeks} (n=4, mean±SEM, $^{\Psi}p<0.001$). No significant change was seen in HMGB1 distribution when the SHR was compared with the WKY by the 20^{th} week (n=4, scale bar=20μm). (**B**) Quantification of the relative distribution of HMGB1 in the nucleus and cytoplasm of PVN neurons in SHR and WKY rats (4 and 20 weeks). (**C**) Representative confocal images showing the localization of HMGB1 in the nucleus of PVN neurons in 4 and 20 weeks old SHR (n=5, scale bar = 5μm). The distribution of extranuclear HMGB1 increased in the SHR at 20 weeks when compared with SHR^{4weeks}.

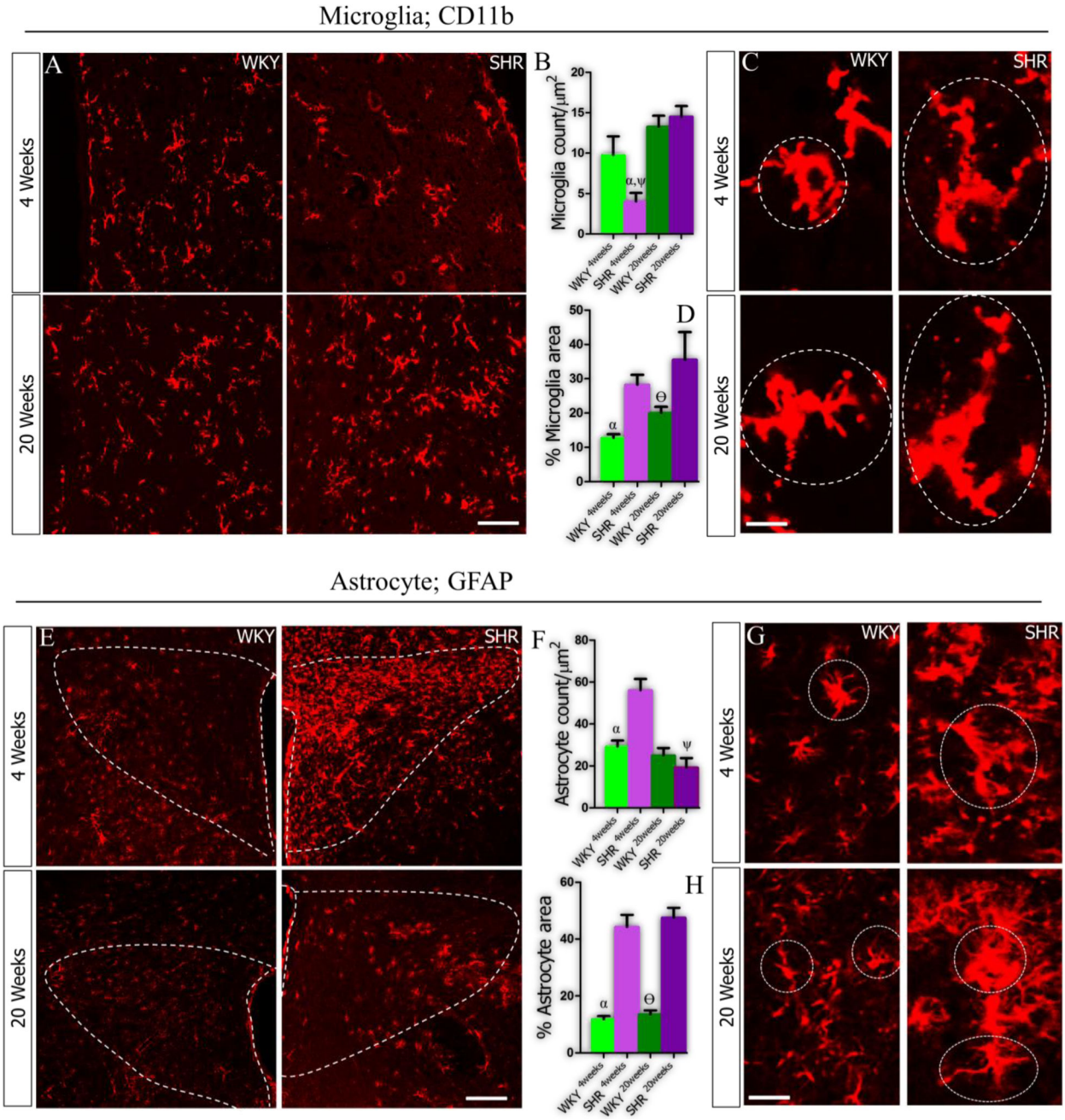

Figure 3.

A-H| Distribution of microglia (CD11b) and astrocytes (GFAP) in the PVN of SHR and WKY rats at 4 and 20 weeks. (**A**) Significantly lower microglia count was recorded in the PVN of SHR ($^{\alpha}p<0.05$) at 4 weeks when compared with WKY (n=6, scale bar =20μm). By the 20^{th} week, the SHR showed a profound increase in microglia count when compared to the SHR^{4weeks} ($^{\Psi}p<0.001$). (**B**) Bar chart depicting the distribution of microglia in the PVN of SHR and WKY rats. (**C**) Higher magnification representative confocal images showing the filed area covered by microglia cells in the PVN. (**D**) Although the microglia count did not change significantly in the SHR, we observed a prominent increase in the microglia field

versus the WKY ($^{\alpha}p<0.01$; scale bar =3μm). Similarly, by the 20th week, the SHR maintained a wider microglia field when compared with the WKY ($^{\theta}p<0.05$). (**E**) Representative confocal images showing the distribution of astrocytes in the PVN of SHR and WKY rats. (**F**) Statistical analysis (*T-test*) showed that GFAP positive cells (astrocytes) increased significantly in the PVN of SHR when compared with the WKY by the 4th week ($^{\alpha}p<0.001$; scale bar =20μm), and was reduced by the 20th week ($^{\Psi}p<0.01$). (**G-H**) The SHR showed a wider astrocyte filed area by the 4th and 20th week when compared with the WKY ($^{\alpha}p<0.001$ and $^{\theta}p<0.001$; scale bar =5μm)

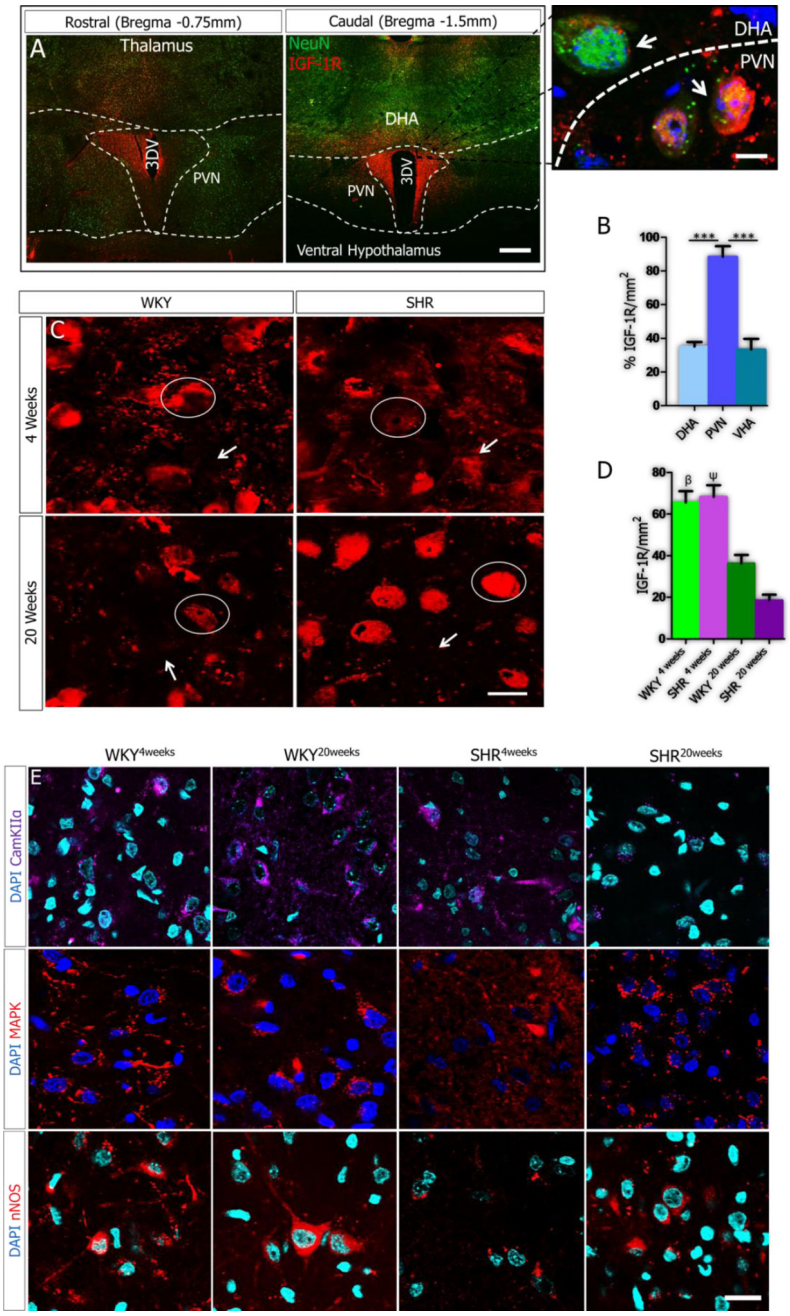

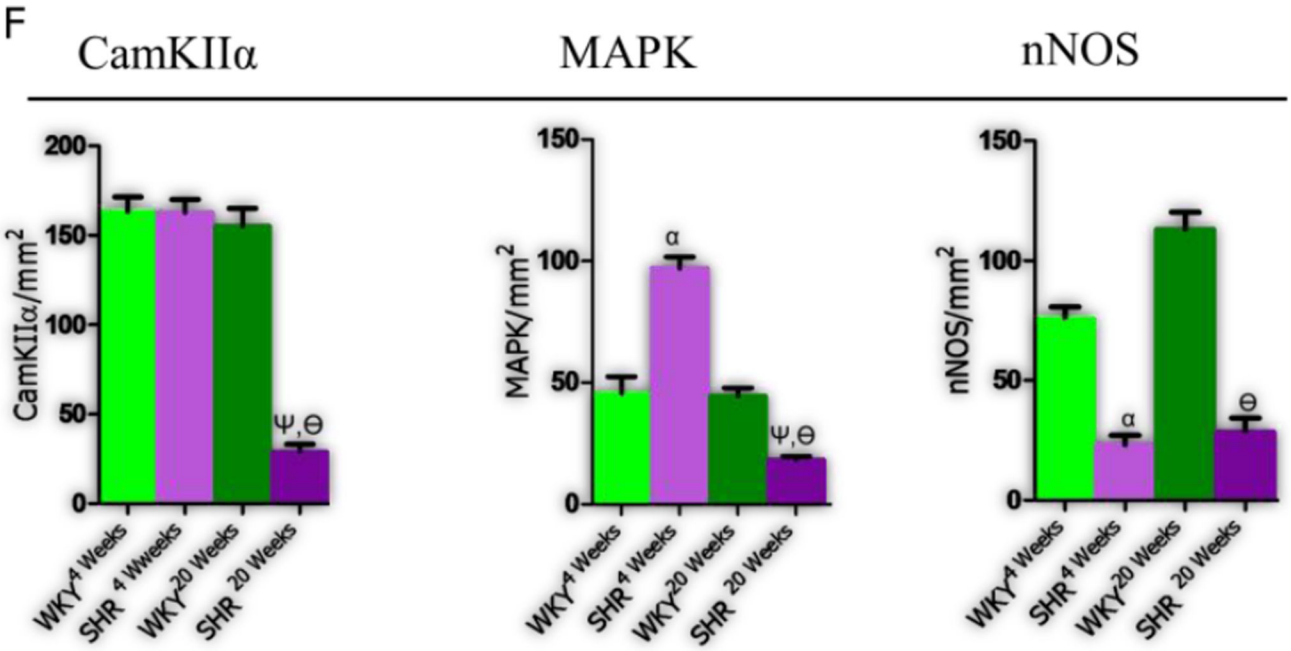

Figure 4.

A-F| IGF-1R expression in downregulated in the PVN of SH and WKY rats with age. (**A-B**) Confocal image showing the preferential expression of IGF-1R in the PVN of rats when compared with the dorsal (DHA) and ventral hypothalamic areas (VHA) (n=3, scale bar=50μm; $p<0.001$) (**C**) Representative confocal images for the expression of IGF-1R in the PVN of SH and WKY rats at 4 and 20 weeks (n=6). No significant change was observed in IGF-1R expression when the SHR was compared with WKY at 4 weeks (scale bar=20μm, 5μm). A profound decrease in IGF-1R expression was seen in the PVN of the $WKY^{20weeks}$ when compared with the WKY^{4weeks} PVN (n=6, mean±SEM, $^{\beta}p<0.05$). Similarly, IGF-1R decreased in the PVN of $SHR^{20weeks}$ when compared with SHR^{4weeks} (n=6, mean±SEM, $^{\Psi}p<0.01$). (**D**) Quantitative representation of IGF-1R distribution in the PVN of SHR and WKY rats. (**E**) Change in the expression of IGF-1R-associated signaling molecules (CamKIIα, MAPK/ErK1/ErK2 and nNOS) with age contributes to the progression of synaptic changes in the PVN of SHR (n=6, scale bar=20μm). (**CamKIIα**) No significant change was observed in CamKIIα expression when the SHR was compared with WKY at 4 weeks (n=6). Similarly, no significant change was seen in CamKIIα, with age, in the WKY PVN (WKY^{4weeks} versus $WKY^{20weeks}$). By contrast, an age-dependent depletion of CamKIIα was observed in the PVN of SHR by the 20^{th} week when compared with SHR^{4weeks} (n=6, mean±SEM, $^{\Psi}p<0.001$) and $WKY^{20weeks}$ (n=6, Mean±SEM, $^{\Theta}p<0.001$). (**MAPK/ErK**) MAPK/ErK was over-expressed in the PVN of SHR at 4 weeks; when compared with the WKY (n=6, mean±SEM, $^{\alpha}p<0.001$). The distribution of MAPK/ErK did not change significantly with age in the PVN of WKY rats at 4 and 20 weeks. By contrast, MAPK/ErK decreased significantly with age in the PVN of $SHR^{20weeks}$ when compared with SHR^{4weeks} (n=6, mean±SEM, $^{\Psi}p<0.001$) and $WKY^{20weeks}$ (n=6, mean±SEM, $^{\Theta}p<0.05$). (**nNOS**) No significant change in nNOS was observed with age in the PVN of SHR and WKY from the 4^{th} to 20^{th} week. A profound decrease in nNOS was seen in the SHR when compared with WKY at 4 (n=6, mean±SEM, $^{\alpha}p<0.001$) and 20

weeks (n=6, mean±SEM, $^{\theta}p<0.001$) (scale bar=20μm). (**F**) Statistical (bar graph) representation for the expression of CamKIIα, MAPK/ErK and nNOS in the PVN of SHR and WKY rats.

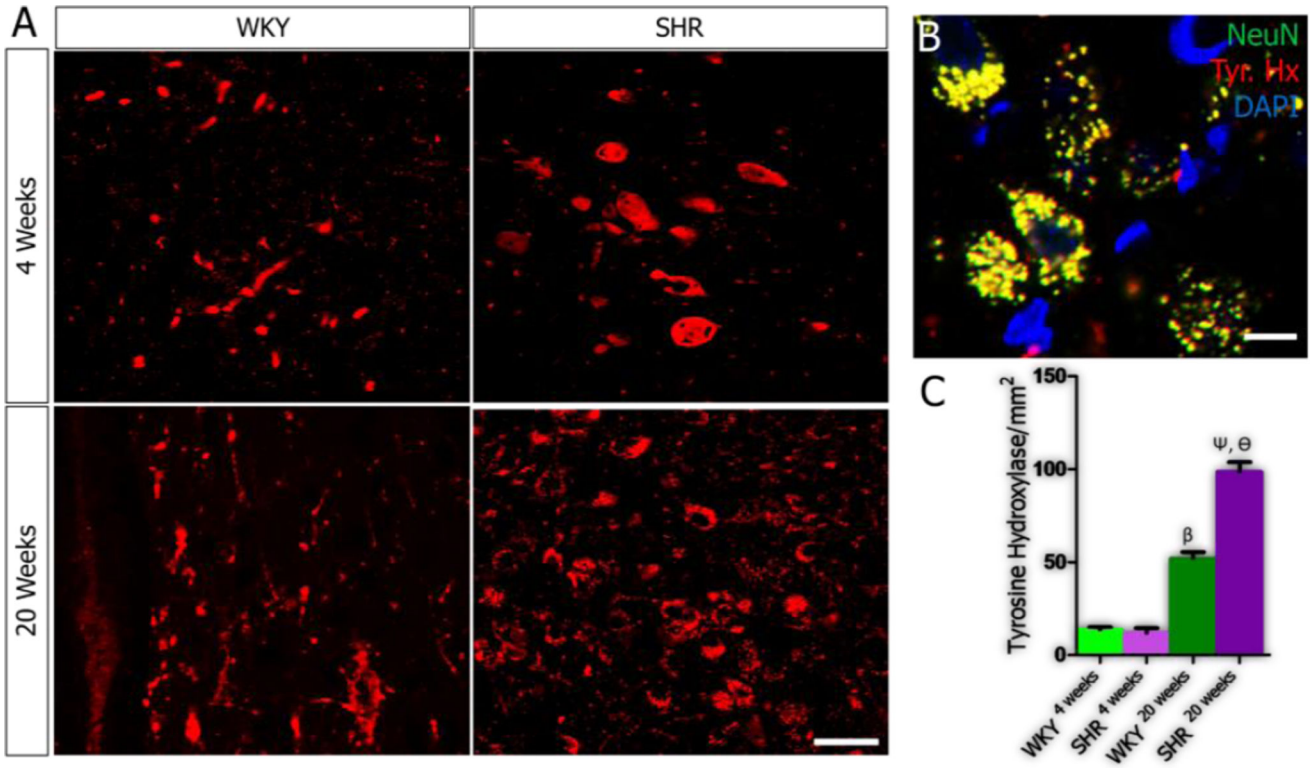

Figure 5.

A-C| Age-dependent change in Tyrosine Hydroxylase in the PVN of SH and WKY rats. (**A**) No significant difference in catecholaminergic activity was seen when tyrosine hydroxylase expression was quantified in the PVN of SHR and WKY at 4 weeks. Catecholaminergic activity increased with age in WKY rats when WKY^{4weeks} was compared with $WKY^{20weeks}$ (n=4, mean±SEM, $^{\beta}p<0.001$). Similarly, an increase in catecholaminergic activity was observed in the PVN of SHR rats from 4 to 20 weeks (n=4, mean±SEM, $^{\Psi}p<0.001$). We observed a more significant increase in the catecholaminergic activity in the PVN of SHR at 20 weeks when compared with WKY (n=4, mean±SEM, $^{\theta}p<0.001$) (scale bar=20μm). (**B**) Representative confocal image showing the co-localization of tyrosine hydroxylase and NeuN (yellow) considered for the quantification of tyrosine hydroxylase and identification of catecholaminergic neurons in the PVN of $SHR^{20weeks}$ (scale bar=5μm). (**C**) One-way ANOVA comparison for tyrosine hydroxylase expression in the PVN of SHR and WKY rats. Data was presented as bar graphs with error bars representing mean±SEM.

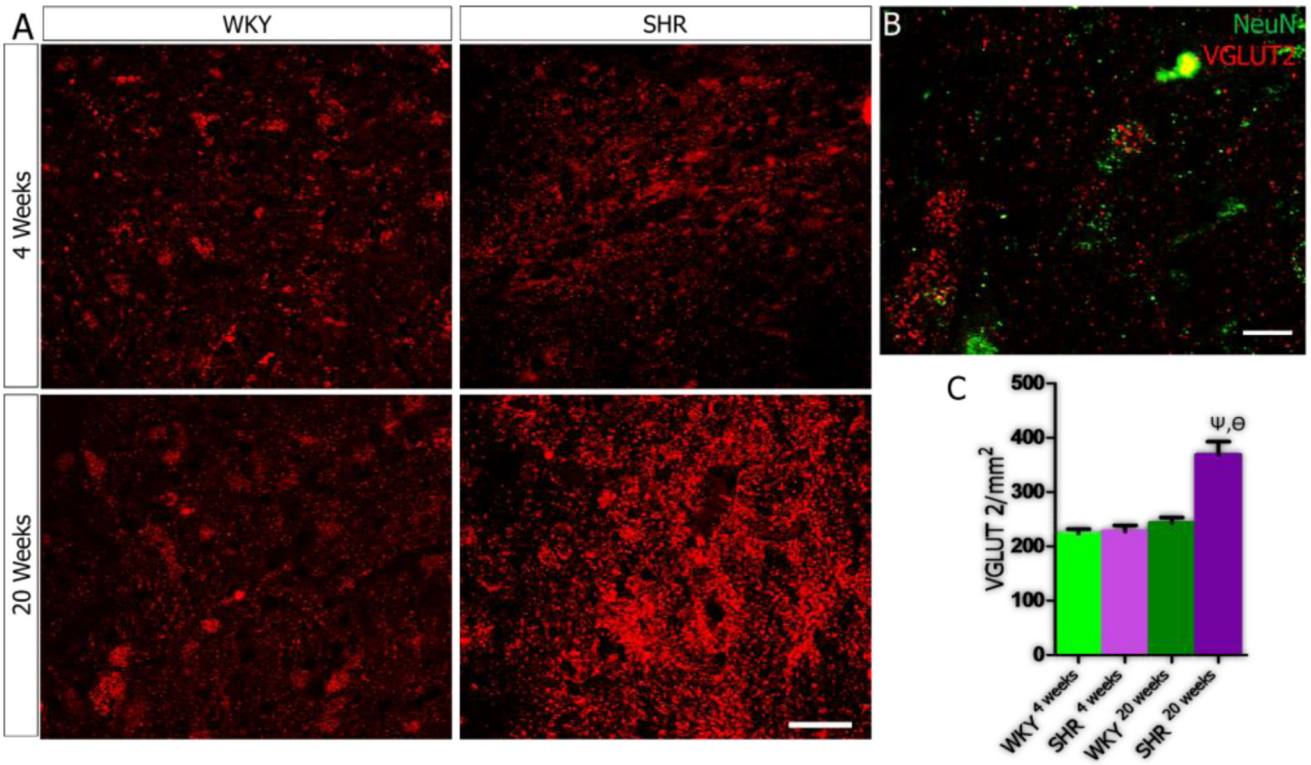

Figure 6.

A-C| VGLUT 2 expression in PVN neurons of SHR. (**A**) No significant change in VGLUT2 expression in the PVN of SHR and WKY rats at 4 weeks. Similarly, VGLUT2 expression did not change with age in the WKY when WKY^{4weeks} was compared with $WKY^{20weeks}$. VGLUT2 expression increased in the PVN of SHR with age when $SHR^{20weeks}$ was compared with $SHR^{4\ weeks}$ (n=4, mean±SEM, $^{\Psi}p<0.001$). Furthermore, VGLUT2 was over-expressed in the $SHR^{20weeks}$ when compared with the WKY (n=4, mean±SEM, $^{\theta}p<0.001$) (scale bar=20μm). (**B**) Higher magnification confocal image showing the co-localization of VGLUT2 and NeuN in the PVN of $SHR^{20weeks}$ (scale bar=5μm). (**C**) Statistical analysis and bar graph showing the distribution of VGLUT2 in the PVN of SHR and WKY rats.

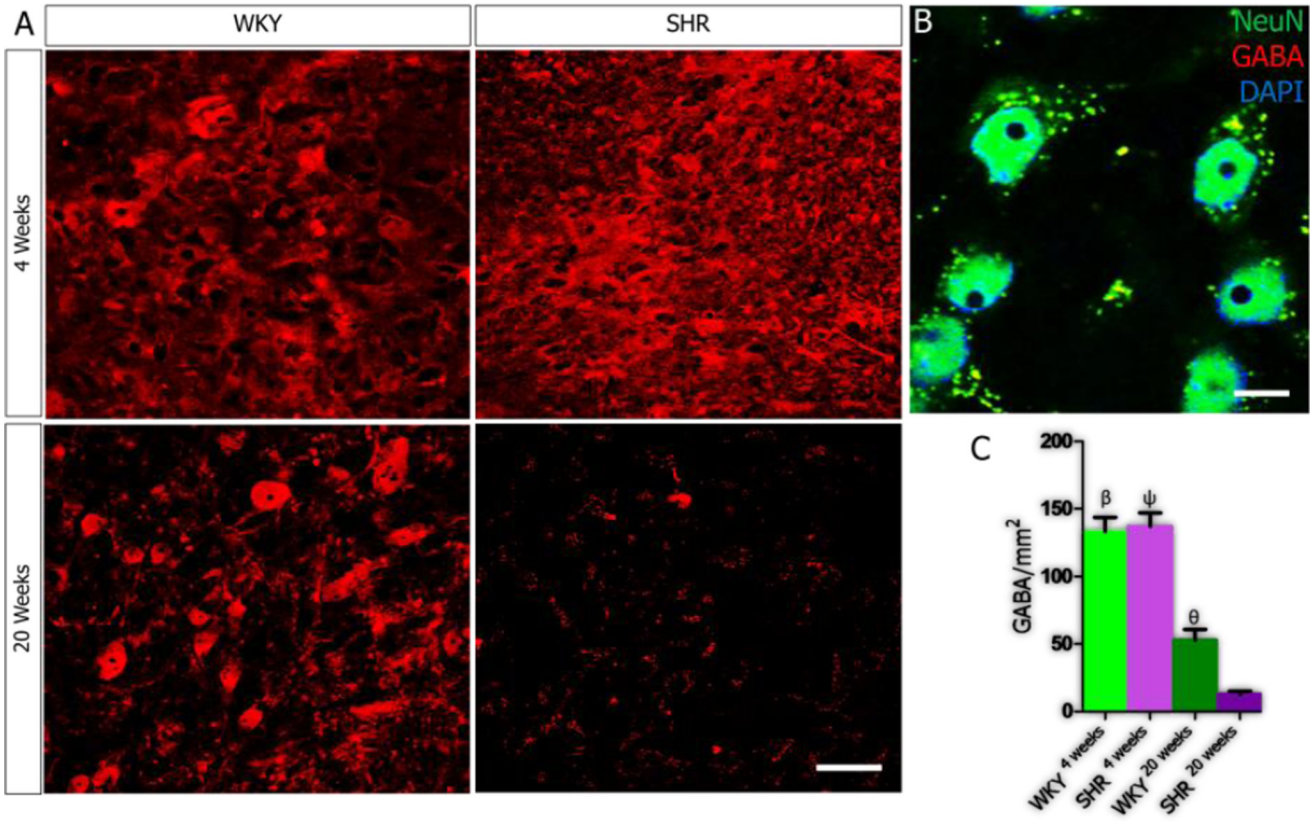

Figure 7.

A-C| Depletion of GABA in the PVN of SHR. (**A**) At 4 weeks, no significant change in GABA was observed when the SHR was compared with the WKY. GABA reduced prominently in the PVN of WKY rats with age. This was seen as a significant decrease when WKY^{4weeks} was compared with $WKY^{20weeks}$ (n=5, mean±SEM, $^{\beta}p<0.001$). Similarly, a significant reduction in GABA was seen in the PVN of SHR with age; when SHR^{4weeks} was compared with $SHR^{20weeks}$ (n=4, mean±SEM, $^{\Psi}p<0.001$). Although GABA reduced in the WKY and SHR with age, we recorded a more significant decrease in the PVN of SHR versus the WKT at 20 weeks (n=4, mean±SEM, $^{\theta}p<0.05$) (**B**) Higher magnification confocal image showing the co-localization of GABA and NeuN in the PVN (scale bar=5μm). (**C**) Statistical analysis and bar graph representation of GABA expression in the PVN of SHR and WKY rats.

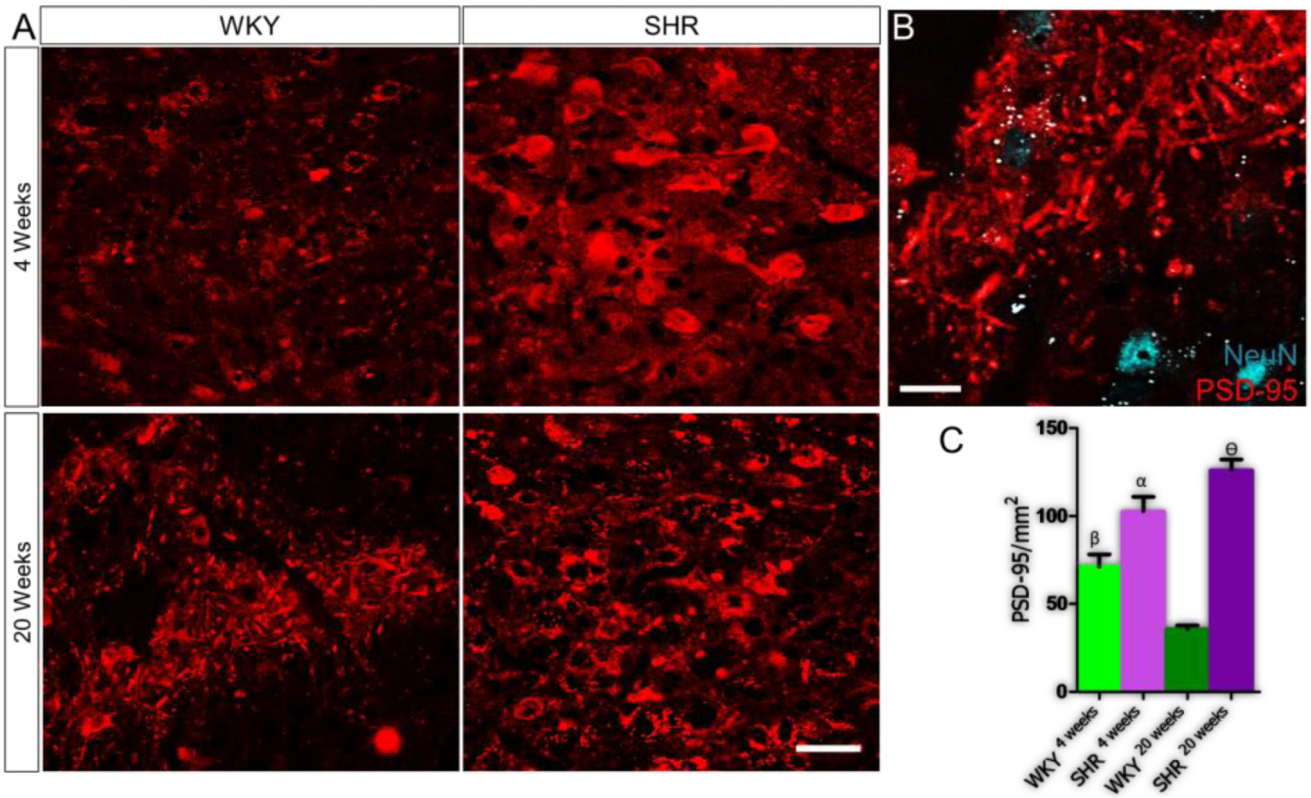

Figure 8.

A-C| Post-synaptic modifications occur with age in the PVN of SHR and WKY rats. (**A**) PSD-95 expression increased significantly in the SHR when compared with the WKY by the 4^{th} week (n=5, mean±SEM, $^{\alpha}p<0.05$). Furthermore, PSD-95 decreased with age in the $WKY^{20\ weeks}$ PVN; when compared with $WKY^{4\ weeks}$ (n=4, mean±SEM, $^{\beta}p<0.05$). PSD-95 increased significantly with age in the SHR, when compared with the WKY at 20 weeks (n=4, mean±SEM, $^{\theta}p<0.001$) (scale bar=20μm). (**B**) Higher magnification confocal image showing the distribution of post-synaptic densities in the PVN (scale bar=5μm). (**C**) Statistical analysis and bar graph representation of PSD-95 distribution in the PVN of SHR and WKY rats.

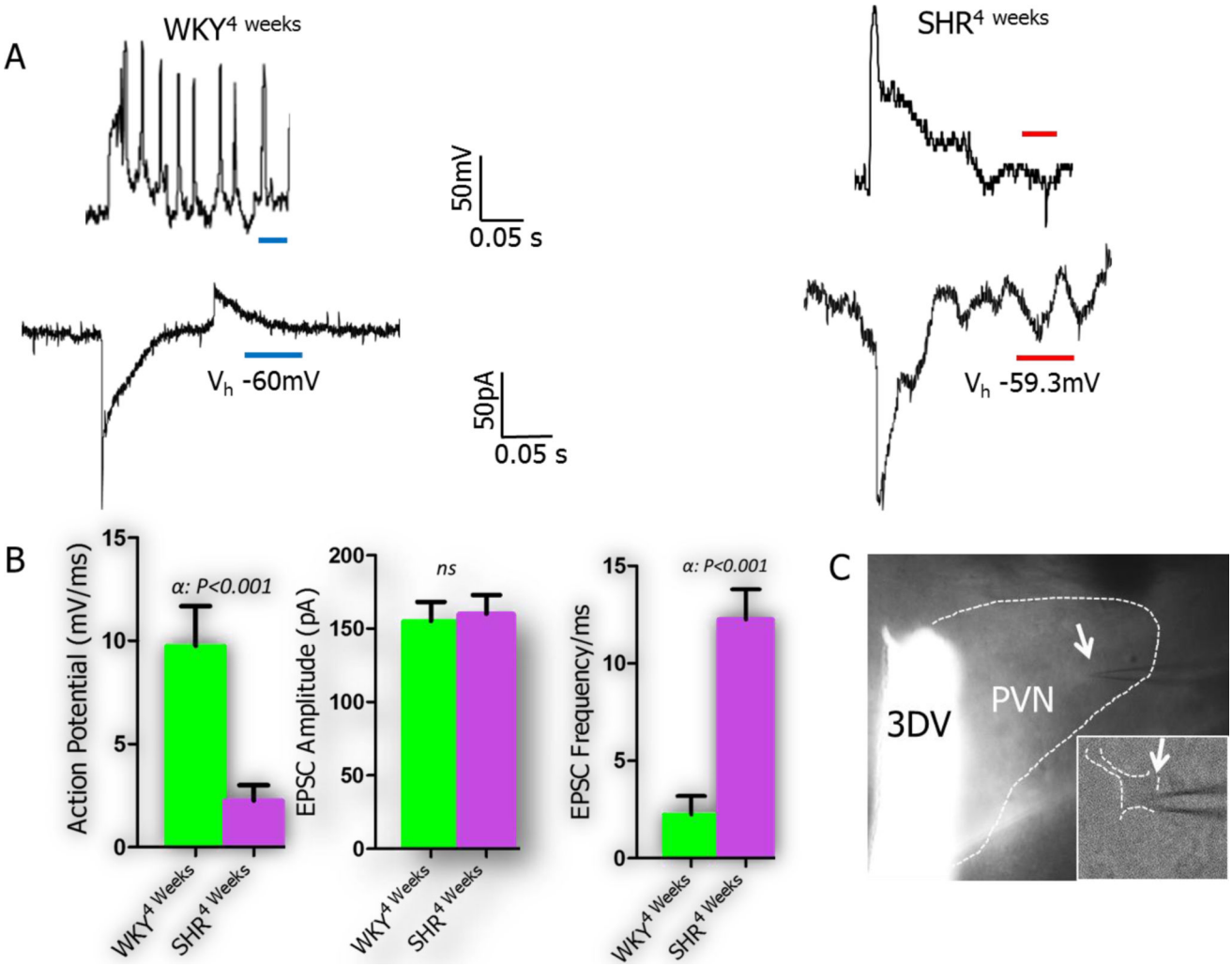

Figure 9.

A-C| Synaptic dysfunction occurs early in the PVN of SHR. (**A**) Whole-cell perforated patch recording of EPSCs in current and voltage clamp mode. SHR PVN neurons (n=9 cells) showed spontaneous neural activity characterized by abnormal and repetitive inward currents when compared with the WKY (n=5 cells). (**B**) The PVN neurons of SHR^{4weeks} showed a defective baseline action potential versus the WKY in current clamp (mV). In voltage clamp mode, the frequency of inward currents (EPSC) was significantly higher in SHR versus the WKY (mean±SEM, $^{\alpha}p<0.001$); although the amplitude was unchanged. (**C**) Phase-contrast image showing the electrode placement (arrow) above a PVN neuronal cell body.

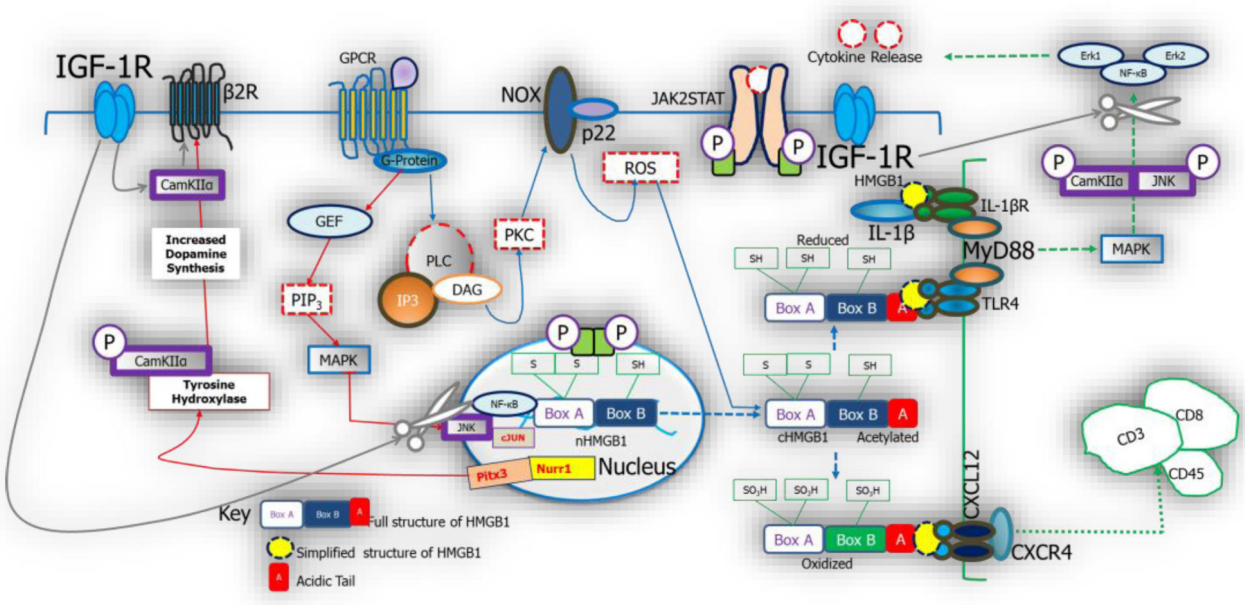

Figure 9.

Schematic illustration of possible interactions between PVN inflammation and sympathoexcitation in spontaneously hypertensive rats. The activation of HMGB1 occurs as a result post-translational modifications which involves acetylation of the box B components. This is also associated with the cytoplasmic translocation of the protein. Depending on its redox state, HMGB1 either binds to TLR4 or CXCR4 to promote inflammation or leucocyte migration in the nervous system. The activities of MAPK in HMGB1 signaling facilitate the release of downstream molecules (NF-κB). Furthermore, it increases the release of transcriptomes (Nurr1 and Pitx3; not investigated), which favors the production of tyrosine hydroxylase (catecholaminergic activity). MAPK also increases the presynaptic releases of glutamate (vesicular glutamate activity) and control catecholaminergic neurotransmission; thus affecting sympathoexcitation. In a separate pathway, HMGB1 promotes the depletion of nNOS and depletes the “inhibitory” GABAergic system; further promoting sympathoexcitation. Change in the expression pattern of IGF-1R may play important roles in the control of inflammation and sympathoexcitation. Through the activation of CamKIIα, IGF-1R reduces the rate at which HMGB1 activates NF-κB. Similarly, CamKIIα phosphorylates MAPK/Erk1/Erk2 to reduce the progression of inflammation mediated through TLR4. Ultimately, IGF-1R and its secondary messenger molecule (CamKIIα) interact with catecholaminergic receptors at synaptic terminals to exert control on the activation of ionotropic glutamatergic receptors.